U-Th-Pb geochronology of the Coast Mountains batholith in north-coastal British Columbia: Constraints on age and tectonic evolution

G. Gehrels[1,†], M. Rusmore[2], G. Woodsworth[3], M. Crawford[4], C. Andronicos[5], L. Hollister[6], J. Patchett[1], M. Ducea[1], R. Butler[7], K. Klepeis[8], C. Davidson[9], R. Friedman[10], J. Haggart[3], B. Mahoney[11], W. Crawford[4], D. Pearson[1], and J. Girardi[1]

[1]*Department of Geosciences, University of Arizona, Tucson, Arizona 85721, USA*
[2]*Department of Geology, Occidental College, Los Angeles, California 90041, USA*
[3]*Geological Survey of Canada, Vancouver, British Columbia V6B-5J3, Canada*
[4]*Department of Geology, Bryn Mawr College, Bryn Mawr, Pennsylvania 19010, USA*
[5]*Department of Earth and Atmospheric Sciences, Cornell University, Ithaca, New York 14853, USA*
[6]*Department of Geosciences, Princeton University, Princeton, New Jersey 08544, USA*
[7]*Department of Chemistry and Physics, University of Portland, Portland, Oregon 97203, USA*
[8]*Department of Geology, University of Vermont, Burlington, Vermont 05405, USA*
[9]*Department of Geology, Carleton College, Northfield, Minnesota 55057, USA*
[10]*Department of Earth and Ocean Sciences, University of British Columbia, Vancouver, British Columbia V6T 1Z4, Canada*
[11]*Department of Geology, University of Wisconsin, Eau Claire, Wisconsin 54702, USA*

ABSTRACT

Previously published and new U-Pb geochronologic analyses provide 313 zircon and 59 titanite ages that constrain the igneous and cooling history of the Coast Mountains batholith in north-coastal British Columbia. First-order findings are as follows:

(1) This segment of the batholith consists of three portions: a western magmatic belt (emplaced into the outboard Alexander and Wrangellia terranes) that was active 177–162 Ma, 157–142 Ma, and 118–100 Ma; an eastern belt (emplaced into the inboard Stikine and Yukon-Tanana terranes) that was active ca. 180–110 Ma; and a 100–50 Ma belt that was emplaced across much of the orogen during and following mid-Cretaceous juxtaposition of outboard and inboard terranes.

(2) Magmatism migrated eastward from 120 to 80 (or 60) Ma at a rate of 2.0–2.7 km/Ma, a rate similar to that recorded by the Sierra Nevada batholith.

(3) Magmatic flux was quite variable through time, with high (>35–50 km^3/Ma per km strike length) flux at 160–140 Ma, 120–78 Ma, and 55–48 Ma, and magmatic lulls at 140–120 Ma and 78–55 Ma.

(4) High U/Th values record widespread growth (and/or recrystallization) of metamorphic zircon at 88–76 Ma and 62–52 Ma.

(5) U-Pb ages of titanite record rapid cooling of axial portions of the batholith at ca. 55–48 Ma in response to east-side-down motion on regional extensional structures.

(6) The magmatic history of this portion of the Coast Mountains batholith is consistent with a tectonic model involving formation of a Late Jurassic–earliest Cretaceous magmatic arc along the northern Cordilleran margin; duplication of this arc system in Early Cretaceous time by >800 km (perhaps 1000–1200 km) of sinistral motion (bringing the northern portion outboard of the southern portion); high-flux magmatism prior to and during orthogonal mid-Cretaceous terrane accretion; low-flux magmatism during Late Cretaceous–Paleocene dextral transpressional motion; and high-flux Eocene magmatism during rapid exhumation in a regime of regional crustal extension.

INTRODUCTION

The Coast Mountains batholith (also known as the Coast Plutonic Complex) consists of Jurassic through Tertiary plutonic rocks and associated metamorphic pendants and screens that extend along the west coast of northern North America. These plutonic and metamorphic rocks can be traced continuously for over 1700 km, from northern Washington through coastal British Columbia and southeast Alaska into southwestern Yukon (Fig. 1). The width of the batholith ranges from ~50 to ~150 km.

The Coast Mountains batholith provides an important laboratory for studying processes of batholith formation and continental margin evolution because (1) it is one of the largest coherent plutonic masses on Earth, (2) plutons presently exposed at the surface were emplaced at a wide range of crustal levels, from >25 km depth to subvolcanic, (3) igneous rocks range in composition from gabbro through leucogranite (although most are tonalitic), (4) magmatism occurred for over 100 Ma, during which plate motions along the west coast of North America changed dramatically, and (5) plutons were generated and emplaced in proximity to, and during motion along, major thrust, normal, and strike-slip fault systems, some of which form boundaries between distinct terranes. These features provide opportunities to investigate genetic linkages among plutonism, metamorphism, exhumation, terrane accretion, displacement on shear zones, and changes in plate motion.

Our research has been conducted as part of the ACCRETE, BATHOLITHS, and related projects, which involve regional mapping, structural and stratigraphic analyses, geochemistry, geochronology, thermochronology, petrology, and both active and passive seismology. These projects are focused on the Coast Mountains batholith in north-coastal British Columbia and southernmost southeast Alaska (Fig. 1). The purpose of this paper is to summarize the

[†]E-mail: ggehrels@email.arizona.edu

GSA Bulletin; September/October 2009; v. 121; no. 9/10; p. 1341–1361; doi: 10.1130/B26404.1; 12 figures; 1 table; Data Repository item 2009054.

For permission to copy, contact editing@geosociety.org
© 2009 Geological Society of America

U-Pb geochronologic information that has been acquired during these projects and prior investigations, integrate these data with results from complementary structural, petrologic, and geochemical data, and use this information to constrain the tectonic evolution of this portion of the Coast Mountains batholith.

This paper presents 84 new U-Pb zircon ages and 41 new U-Pb titanite ages, from 87 samples, and integrates these new ages with geochronologic information that has been generated and reported by numerous other researchers. Most of our samples were collected in an attempt to constrain the ages of the main plutonic components in this portion of the batholith. The available ages are summarized on Figures 2 and 3, which show general age patterns of zircon from plutonic and subordinate volcanic rocks (Fig. 2A) and titanite from plutonic rocks (Fig. 3). The base maps for this compilation are from Wheeler and McFeely (1991) for geologic units and Wheeler et al. (1991) for terranes. Primary aspects of these units and terranes are described in the Appendix.

Zircon ages are binned on Figure 2A according to the main magmatic pulses apparent on an age-distribution diagram (Fig. 2B). This diagram sums the age-probability distribution (e.g., 143 ± 2 Ma) from all samples (Fig. 2A) and plots the summed probabilities as a continuous curve. The distribution of ages is also shown on a histogram (Fig. 2B), but the age divisions on Figure 2A were determined from the age-distribution curve because it provides a more complete description of the ages and uncertainties.

Maps showing all of the ages and sample numbers are included in the accompanying GSA Data Repository (see Figs. DR1–DR3).[1] For samples that are reported for the first time in this paper, geologic and geochronologic information is provided in Table DR1 and Figures DR4–DR217 (see footnote 1). Ages and supporting information for the entire data set are reported in Table DR2 (see footnote 1).

One of the fundamental assumptions in this analysis is that all of the first-order igneous suites in the region have been recognized and characterized geochronologically. Fortunately, much of the geochronologic work in the region has been done in an effort to determine ages for the main plutonic suites, and most of the samples reported herein (Table DR2, see footnote 1) were collected specifically for this purpose. Two igneous suites that are under-represented in

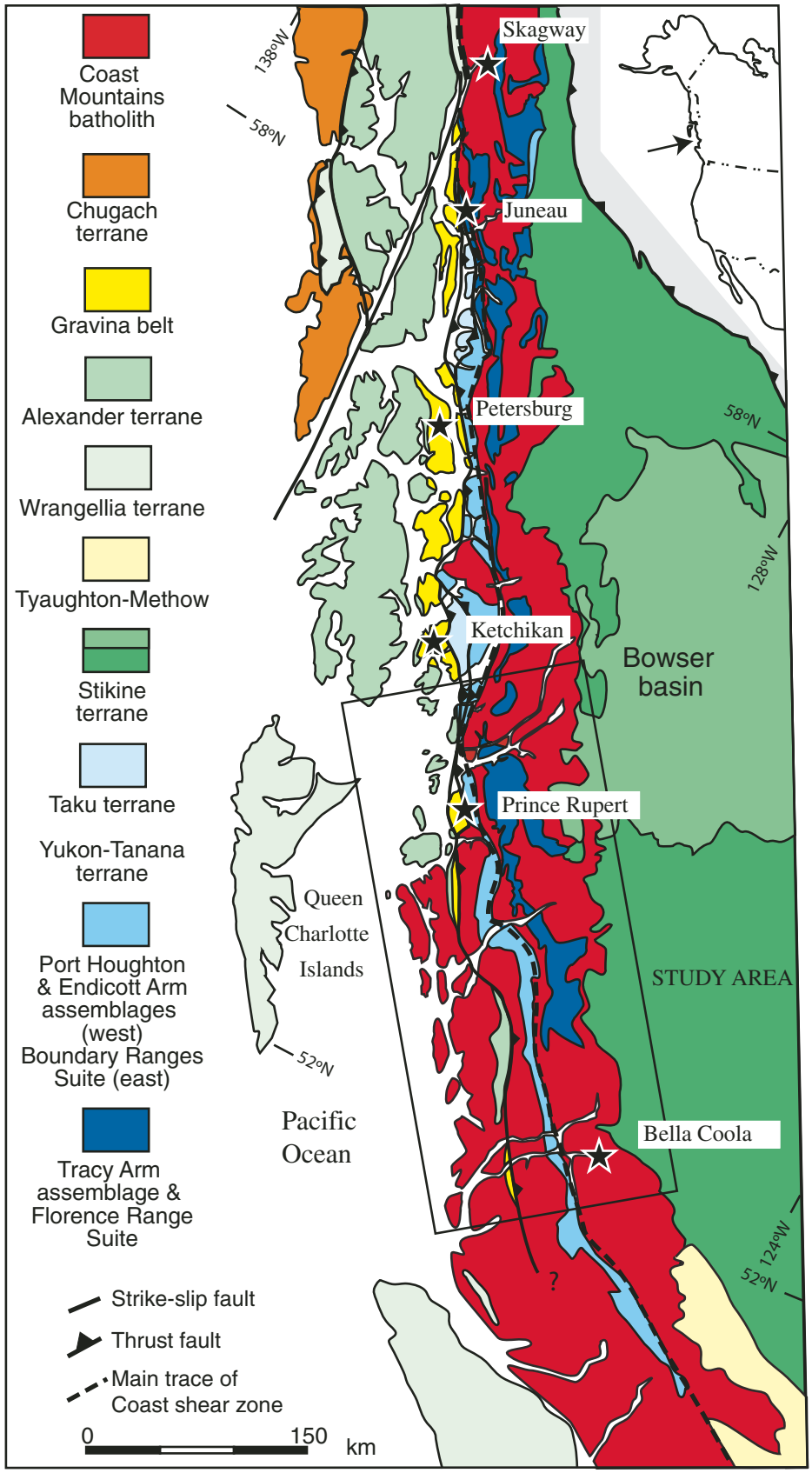

Figure 1. Geologic framework of the Coast Mountains batholith (adapted from Wheeler and McFeely, 1991; Wheeler et al., 1991).

[1]GSA Data Repository item 2009054, two tables and 217 figures that include geologic and U-Pb geochronologic information, is available at http://www.geosociety.org/pubs/ft2009.htm or by request to editing@geosociety.org.

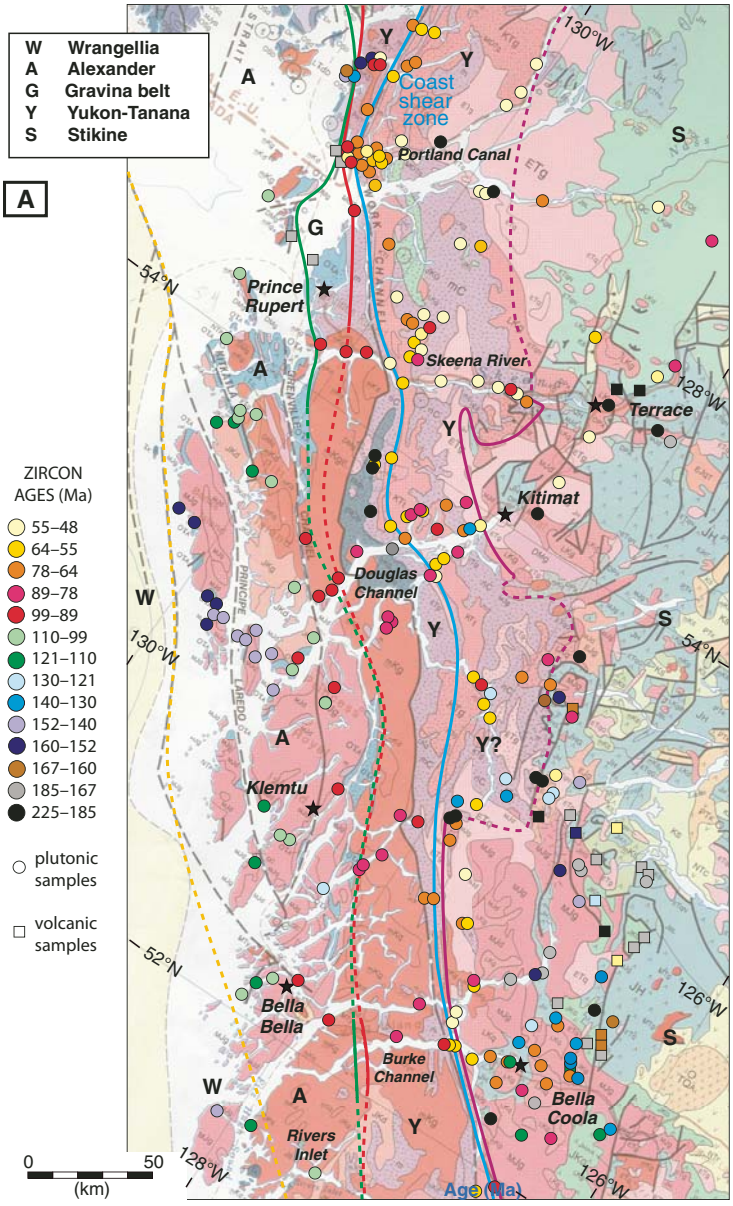

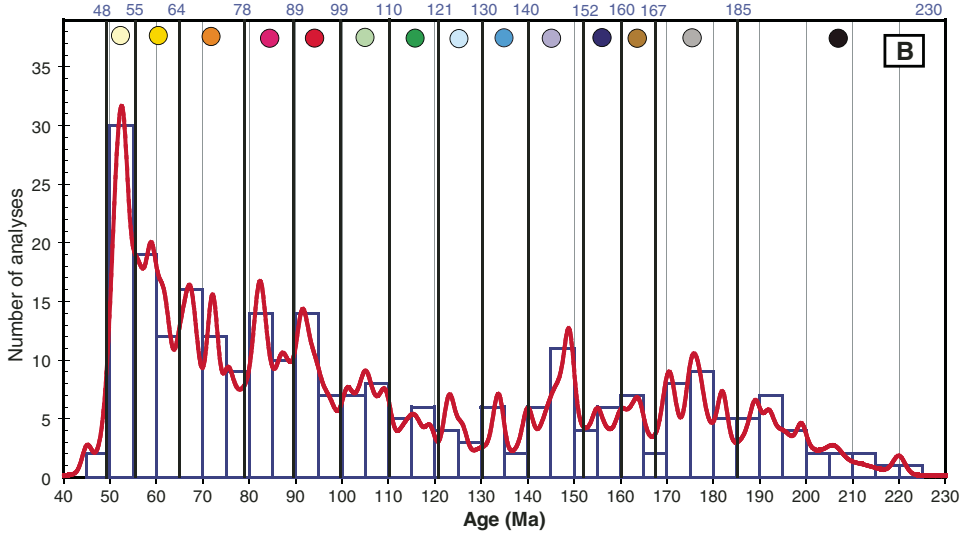

Figure 2. (A) Age range and approximate location of U-Pb (zircon) samples. Background geology is from Wheeler and McFeely (1991) and Wheeler et al. (1991) (see the Appendix for definition of map units). Ages of plutonic rocks are shown with circles; ages of volcanic rocks are shown with squares. Ages and sample numbers are shown on Figures DR1–DR2 and listed in Table DR2 (see text footnote 1). (B) Relative age-distribution plot of U-Pb (zircon) ages. The age-distribution curve was constructed by summing the age distributions of all 268 U-Pb (zircon) ages in the study area that are between 230 and 40 Ma. Boundaries of age bins were selected at ~10 Ma intervals, adjusted for age-distribution minima.

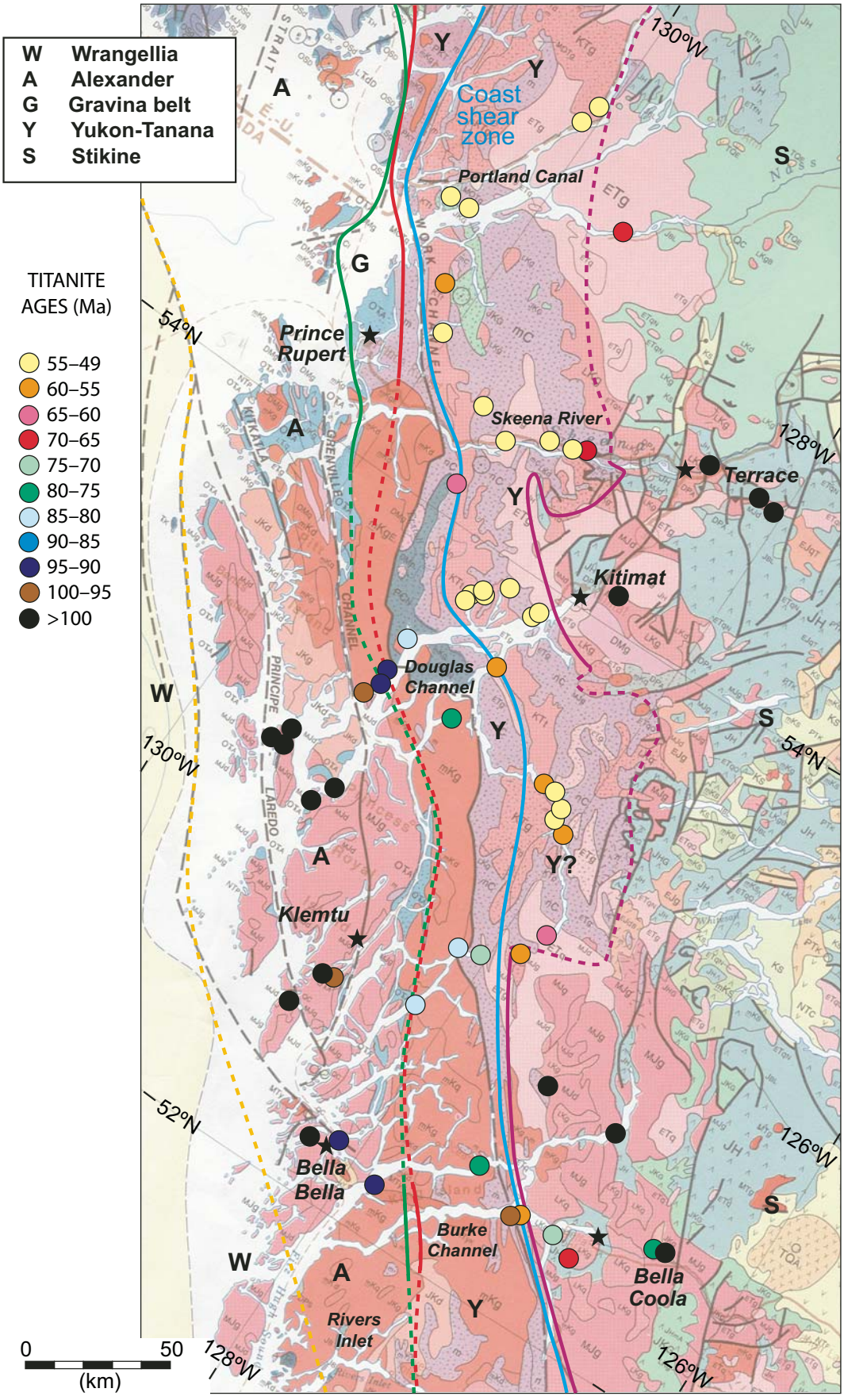

Figure 3. Age range and approximate location of U-Pb (titanite) samples (see the Appendix for definition of map units). Ages and sample numbers are shown on Figures DR1 and DR3 and listed in Table DR2 (see text footnote 1).

this analysis, however, include migmatitic components in central portions of the batholith, and widespread mafic dikes of known and suspected Tertiary age. The impact of under-representation of these components is discussed later.

An additional concern is whether sampling has been biased toward particular igneous suites, such that the final set of ages is not an accurate reflection of the volume of igneous rock generated through time. This is certainly the case, such that a histogram or age-distribution curve of all ages (Fig. 2B) does not reflect true magmatic flux. As described here, we have attempted to remove this bias by using existing geologic mapping to reconstruct the volumes of each plutonic suite. When coupled with the available age information, data are interpreted to yield a more robust magmatic flux history.

GEOCHRONOLOGIC METHODS

Most of the analyses presented for the first time herein were conducted by laser-ablation–inductively coupled plasma–mass spectrometry (LA-ICP-MS) at the Arizona LaserChron Center (www.geo.arizona.edu/alc) utilizing methods described by Gehrels et al. (2008). These analyses involved ablation of zircon with a New Wave DUV193 Excimer laser (operating at a wavelength of 193 nm) using a spot diameter of 10–35 μm and a pit depth ranging between 4 and 15 μm. The ablated material was carried with helium gas into the plasma source of a GV Instruments Isoprobe, which was equipped with a flight tube of sufficient width that U, Th, and Pb isotopes were measured simultaneously. All measurements were made in static mode using Faraday detectors with 1×10^{11} Ω resistors for ^{238}U, ^{232}Th, ^{208}Pb, and ^{206}Pb, a Faraday detector with a 1×10^{12} Ω resistor for ^{207}Pb, and an ion-counting channel for ^{204}Pb. Ion yields were ~1 mv per ppm using a 35 μm beam and an ablation rate of 1 μm/s. Most analyses consisted of one 12 s integration on peaks with the laser off (for backgrounds), twelve 1 s integrations with the laser firing, and a 30 s delay to purge the previous sample and prepare for the next analysis. Age mapping analyses (Gehrels et al., 2008; Johnston et al., 2009) involved counting for 10 s on backgrounds and ~8 s on peaks, and isotope ratios were calculated from total ion counts rather than a series of integrations.

For each analysis, the errors in determining ^{206}Pb/^{238}U and ^{206}Pb/^{204}Pb resulted in a measurement error of ~1%–2% (at 2σ level) in the ^{206}Pb/^{238}U age. The errors in measurement of ^{206}Pb/^{207}Pb and ^{206}Pb/^{204}Pb also resulted in ~1%–2% (2σ) uncertainty in age for grains older than 1.0 Ga, but errors are substantially larger for younger grains due to lower intensity of the ^{207}Pb signal and higher age sensitivity of ^{206}Pb/^{207}Pb. Common Pb correction was accomplished by using the measured ^{204}Pb and assuming an initial Pb composition from Stacey and Kramers (1975) (with uncertainties of 1.0 for ^{206}Pb/^{204}Pb and 0.3 for ^{207}Pb/^{204}Pb).

Interelement fractionation of Pb/U was calibrated by comparison (generally every fourth measurement) with a Sri Lanka zircon standard (known age of 563.5 ± 3.2 Ma; Gehrels et al., 2008) or Bear Lake Road titanite standard (1050 ± 3 Ma; John Aleinikoff and Mark Schmitz, 2004, written commun.). The uncertainty resulting from the calibration correction is generally ~1% (2σ) for both ^{206}Pb/^{207}Pb and ^{206}Pb/^{238}U ages.

In most cases, reported ages were determined from the weighted mean (Ludwig, 2003) of the ^{206}Pb/^{238}U ages of the concordant and overlapping analyses. Analyses statistically excluded from the main cluster are shown in blue on these figures (Figs. DR4–DR217 [see footnote 1]). Two uncertainties are reported on the plots (e.g., Fig. 4A). The smaller uncertainty (labeled "mean") is based on the scatter and precision of the set of ^{206}Pb/^{238}U ages, weighted according to their measurement errors (shown at 1σ). The larger uncertainty (labeled "age"), which is the uncertainty of the reported age, was determined as the quadratic sum of the weighted mean error plus the total systematic error for the set of analyses. The systematic error, which includes contributions from the standard calibration, age of the calibration standard, composition of common Pb, and ^{238}U decay constant, is generally ~1%–2% (2σ).

Our strategy in analyzing zircon was to perform preliminary analyses on interior and exterior portions of crystals to test for age variations. If exterior and interior portions of the crystals yielded similar ages, additional analyses were conducted primarily on outer portions of grains to take advantage of the generally higher U concentration. In such cases, ~20 analyses were conducted, and the final age was determined from the weighted mean of the ^{206}Pb/^{238}U ages. Figure 4A shows such an analysis. Fortunately, most zircons analyzed from the Coast Mountains batholith did not contain inherited components, younger overgrowths, or Pb loss, and the age interpretations are relatively straightforward.

If exterior and interior portions of the crystals yielded dissimilar ages, cathodoluminescence (CL) images were generated, and additional analyses were conducted on homogeneous portions of both interior portions (cores) and exterior portions (rims or tips) of crystals in an effort to resolve the nature of the complexities and thereby determine the crystallization age. In general, thin rims that have high U/Th (e.g., >10–20), high U concentration (e.g., >1000–2000 ppm), and little or no CL oscillatory zonation (Corfu et al., 2003) are interpreted to have formed as a result of metamorphic processes (although see Harley et al. [2007] for cautionary notes on the use of U/Th as a metamorphic indicator). In many cases, these rims truncate zonation in preexisting zircon, suggesting that zircon dissolution, resorption, and/or recrystallization have been important (Hoskin and Schaltegger, 2003; Corfu et al., 2003; Harley et al., 2007). The compositional signature of high U/Th and high U probably results from the general enrichment of U in environments with abundant metamorphic fluids, the preferential purging of Th relative to U during zircon recrystallization, and/or the depletion of Th during the contemporaneous growth of metamorphic monazite (Hoskin and Schaltegger, 2003; Harley et al., 2007).

In contrast, igneous zircon was recognized by the common occurrence of fine oscillatory zonation in CL images (Corfu et al., 2003; Hoskin and Schaltegger, 2003) combined with typical igneous values of U concentration (<1000–2000 ppm) and U/Th (<10–20). The presence of Pb loss was indicated by a correlation between U concentration and age, where higher-U analyses yielded younger ages. As an example of data from a complex zircon system, Figure 4B shows analyses from a sample in which ca. 400 Ma igneous cores have been overgrown by ca. 83 Ma metamorphic rims. In such cases, weighted mean ages were determined for both components, and the age of the domain with igneous characteristics was interpreted to represent the magmatic age. In some cases, geologic relations also helped to determine the domain that records the age of magmatic crystallization (Table DR1, see footnote 1).

In several cases where the complexity was not resolvable using a 25 or 35 μm beam, the beam diameter was decreased to 10 μm (4 μm depth), and many analyses were conducted on a single crystal. As an example, Figure 4C shows the results of an age-mapping analysis in which 148 measurements were conducted on a single crystal, resulting in the recognition of five different episodes of zircon growth. The interpreted ages of each domain are shown in Figure 4D, and textural and isotopic criteria were used to determine the domain that represents the magmatic age.

Titanite ages were determined by LA-ICP-MS utilizing methods similar to those for zircon analysis. The larger uncertainties for titanite ages result from the generally lower U concentrations and higher common Pb contents of titanite compared to zircon, as well as the possible existence of inherited components

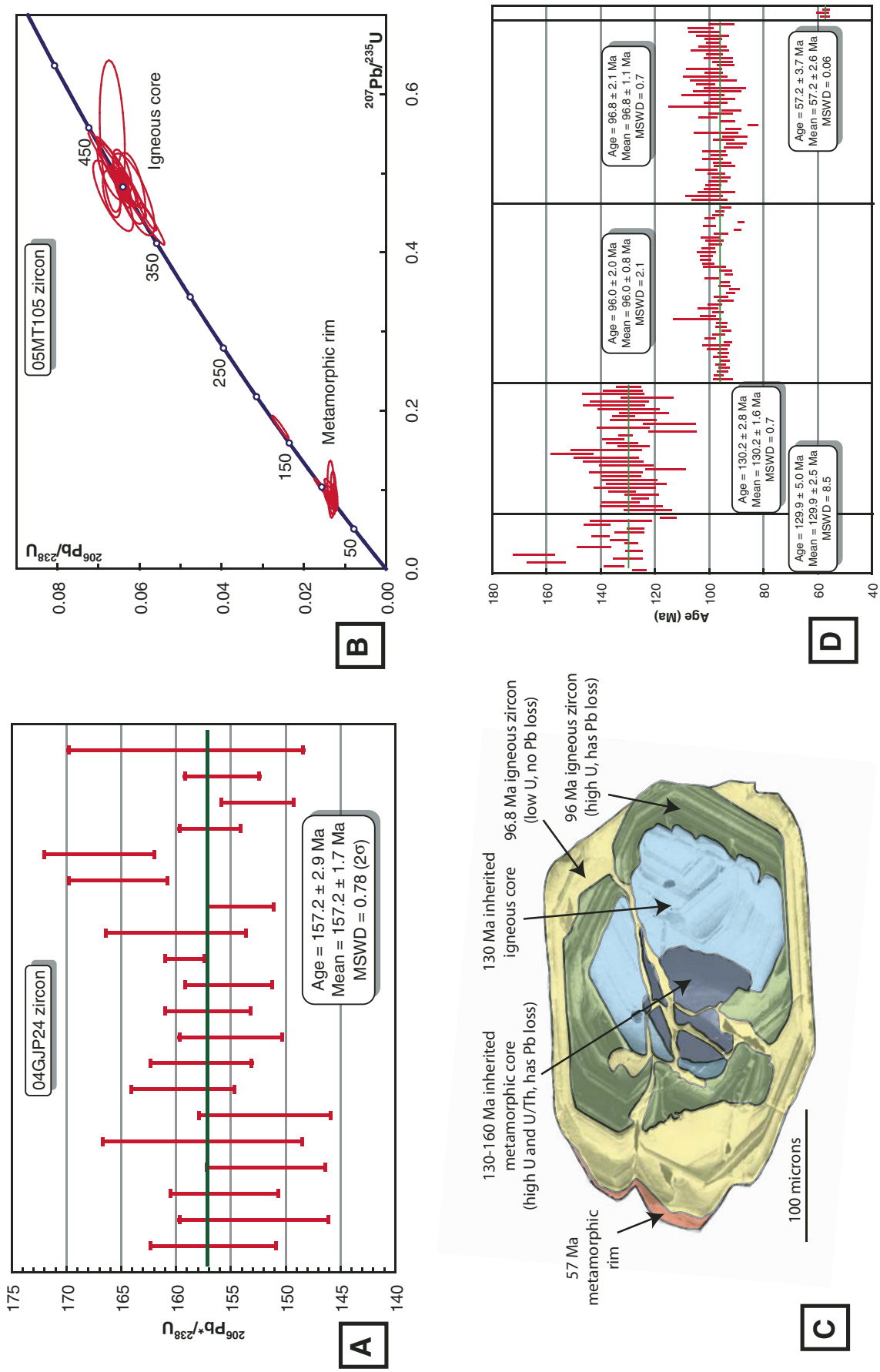

Figure 4. Examples of methods used for determining and interpreting ages from zircons that have simple systematics (A), zircons that contain two different age domains (B), and zircons that have multiple domains that have been analyzed by age mapping (C–D). Uncertainties of individual analyses are shown at 1σ level; uncertainties of pooled analyses are shown at 2σ level. Weighted mean and concordia plots were prepared with Isoplot (Ludwig, 2003). MSWD—mean square of weighted deviates.

and/or Pb loss. In some cases, these factors precluded a reliable age determination. Titanite ages are interpreted to record cooling through ~500 °C (Mattinson, 1982) or perhaps as high as ~650 °C (Pidgeon et al., 1996). In addition to the LA-ICP-MS ages, several samples were analyzed by isotope dilution–thermal ionization mass spectrometry (ID-TIMS), utilizing methods described by Gehrels (2000a).

PREVIOUS WORK

The initial systematic geologic mapping in the study area was conducted by Berg et al. (1988) in southern southeast Alaska, Hutchison (1982) near Prince Rupert, Roddick (1970) along the Skeena River and Douglas Channel, Baer (1973) near Bella Bella and Bella Coola, and Roddick (1994) south of Bella Bella–Bella Coola (Fig. 1). These map sheets were compiled at 1:1,000,000 (Roddick and Hutchison 1974; Hutchison et al., 1973; Tipper et al., 1974) and more recently at 1:2,000,000 (Wheeler and McFeely, 1991).

More recent geologic and/or geochronologic studies in the region were conducted by Douglas (1986), Heah (1990, 1991), Ingram and Hutton (1994), Klepeis et al. (1998), Crawford et al. (1987, 1999, 2000), Saleeby (2000), and Gehrels (2001) in southernmost southeast Alaska and northernmost coastal British Columbia, by Armstrong and Runkle (1979), Harrison et al. (1979), Parrish (1983), van der Heyden (1989, 1992), Gareau (1989, 1991a, 1991b, 1991c), Gehrels et al. (1991), Gareau et al. (1997), Chardon et al. (1999), Andronicos et al. (1999, 2003), Klepeis and Crawford (1999), Gareau and Woodsworth (2000), Hollister and Andronicos (2000, and references therein), Rusmore et al. (2000, 2001, 2005), Butler et al. (2001a, 2002, 2006), Friedman et al. (2001), Chardon (2003), Davidson et al. (2003), and Hollister et al. (2004) in central portions of the study area, and by Rusmore et al. (2001), Farley et al. (2001), Gehrels and Boghossian (2000), van der Heyden (2004), Haggart et al. (2006a, 2006b, 2007), and Mahoney et al. (2007a, 2007b, 2007c, 2007d, 2007e, 2009) to the south. Isotopic and geochemical studies in the study area have been conducted by Smith et al. (1979), Samson et al. (1991a, 1991b), Patchettet et al. (1998), Thomas and Sinha (1999), and Boghossian and Gehrels (2000).

There have also been a number of syntheses outlining igneous, metamorphic, structural, and tectonic aspects of the Coast Mountains batholith in coastal British Columbia (e.g., Armstrong, 1988; Arth et al., 1988; Barker and Arth, 1990; Butler et al., 2001b; Crawford et al., 2005, 2009; Hollister and Andronicos, 1997, 2006; Monger et al., 1982, 1994; Roddick and Hutchison, 1974; Roddick, 1983; Stowell and Crawford, 2000; Woodsworth et al., 1992).

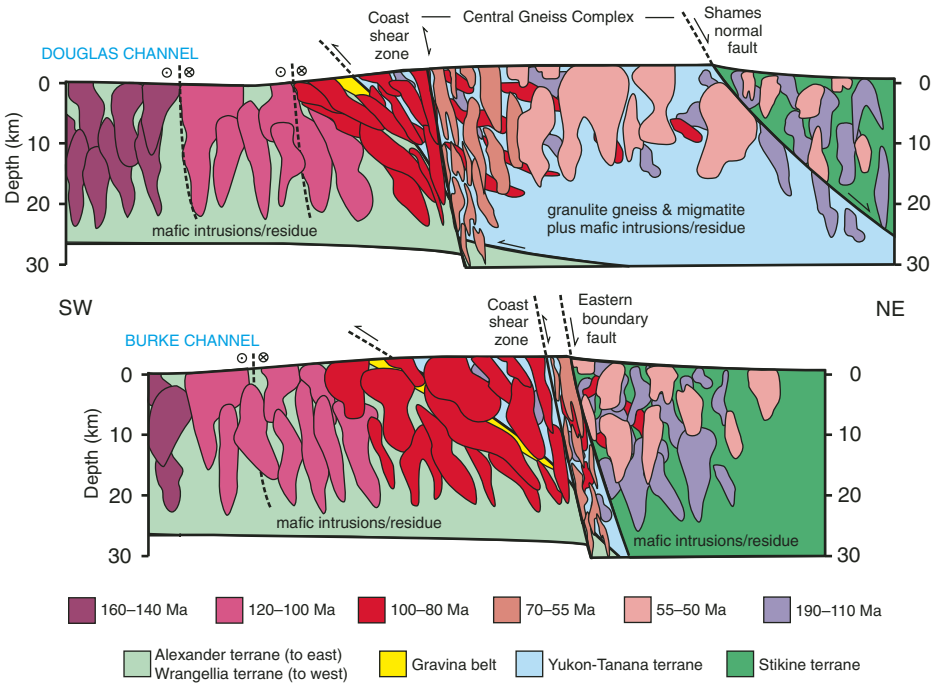

Figure 5. Schematic cross sections of the Coast Mountains batholith at latitudes of Douglas Channel (Kitimat) and Burke Channel (Bella Bella and Bella Coola). Geologic relations are interpreted from Wheeler and McFeely (1991) and this study; crustal thickness is interpreted from Morozov et al. (1998, 2001).

GEOLOGIC SETTING

The aforementioned research provides the basis for the geologic relations shown on Figures 1–3, portrayed schematically in profile view on Figure 5, and described next.

Western Portion of the Coast Mountains Batholith

The western portion of the Coast Mountains batholith is underlain by three distinct belts of plutonic rocks of Late Jurassic, Early Cretaceous, and mid-Cretaceous age. The ages of these bodies decrease systematically eastward (van der Heyden, 1989, 1992; Butler et al., 2006). Their composition also changes eastward, from predominantly quartz diorite on the west to mainly tonalite on the east.

Late Jurassic Plutonic Belt

The westernmost belt, of Late Jurassic (160–140 Ma) age, consists primarily of diorite and quartz diorite, with subordinate gabbro, tonalite, granodiorite, and rare leucogranodiorite. These bodies are not highly deformed, and barometric data suggest emplacement depths of ~10 km (Butler et al., 2006). Metasedimentary country rocks include a distinctive assemblage of quartzite, marble, and pelitic schist, which is referred to as the Banks Island assemblage. These strata are included in the Alexander terrane (Fig. 2A), following Wheeler et al. (1991), although their tectonic affinity remains uncertain (Gehrels and Boghossian, 2000).

Early Cretaceous Plutonic Belt

Toward the east, the plutonic bodies remain quartz dioritic in composition but are dominantly Early Cretaceous in age. Van der Heyden (1989, 1992) interpreted this belt to consist of plutons with ages of ca. 230 Ma, 140–120 Ma, and 120–100 Ma. Analyses of the same bodies by Butler et al. (2006) and herein, however, suggest that all of these bodies are 120–100 Ma in age, and that the older ages reported by van der Heyden (1989, 1992) were compromised by zircon inheritance. Barometric data suggest emplacement depths of ~20 km (Butler et al., 2006). Metasedimentary country rocks consist of early Paleozoic metavolcanic and metaplutonic assemblages overlain by Devonian conglomeratic strata and Triassic volcanic rocks, all of which belong to the Alexander terrane, and overlying Upper Jurassic–Lower Cretaceous

metaturbidites and volcanic rocks of the Gravina belt (Wheeler and McFeely, 1991; Gehrels and Boghossian, 2000; Gehrels, 2001).

Mid-Cretaceous Plutons and Associated Thrust Belt

Farther east, on western slopes of the Coast Mountains, there are large, homogeneous bodies of tonalite and minor quartz diorite and granodiorite. These bodies are quite distinctive because they commonly contain large crystals of epidote and titanite. Crawford and Hollister (1982), Zen (1985), Zen and Hammarstrom (1984), and Crawford et al. (1987) concluded that these bodies were emplaced at depths of >25 km based on the presence of magmatic epidote and on barometric studies of assemblages in their kyanite-bearing metasedimentary host rocks. The Ecstall pluton near Prince Rupert (Hutchison, 1982) is one of these bodies. The available geochronology suggests emplacement during mid-Cretaceous (100–90 Ma) time.

Metasedimentary rocks adjacent to the mid-Cretaceous plutons consist primarily of pelitic schists and metavolcanic rocks of probable mid- and late Paleozoic age (Crawford et al., 2000; Gehrels and Boghossian, 2000; Gehrels, 2001). Metarhyolite layers yield U-Pb ages of 360–280 Ma (Gareau, 1991a; Gareau and Woodsworth, 2000; Gehrels, 2001). These rocks are interpreted to belong to mid-Paleozoic components of the Yukon-Tanana terrane that occur farther north along both the west side (Gehrels et al., 1992; McClelland et al., 1992a) and east side (Currie and Parrish, 1997) of the Coast Mountains, and in a large region of northern British Columbia, Yukon, and eastern Alaska (Colpron et al., 2006). Thin belts of pelitic schist derived from Upper Jurassic–Lower Cretaceous strata of the Gravina belt are also preserved locally.

The mid-Cretaceous plutons are found within a west-vergent thrust belt that can be traced along the western margin of the Coast Mountains for most of its length (Crawford et al., 1987; Rubin et al., 1990; McClelland et al., 1992a; Gehrels et al., 1992). These thrusts juxtapose rocks of the Yukon-Tanana terrane over strata of the Gravina belt in the study area—to the north, strata of the Taku terrane occur as thrust slices between Yukon-Tanana and the Gravina belt. The thrusts also imbricate various units within the Yukon-Tanana terrane and within the Gravina belt. Intrusive relations suggest that emplacement of the mid-Cretaceous plutons accompanied the thrust faulting (Crawford et al., 1987; Himmelberg et al., 2004), and that the plutons may have facilitated motion on the major structures (Hollister and Crawford, 1986).

Axial Portions of the Coast Mountains Batholith

Axial portions of the Coast Mountains are underlain by a heterogeneous assemblage of highly elongate sill-like plutons of foliated tonalite of mostly Paleocene age that are associated with the Coast shear zone, large bodies of generally nonfoliated granodiorite of mostly Eocene age, high-grade (commonly sillimanite-bearing) metasedimentary rocks, orthogneiss, migmatite, and swarms of felsic dikes and sills. These rocks are commonly referred to as the Central Gneiss Complex.

The distribution of these assemblages is consistent from Douglas Channel northward through southeast Alaska, where the Paleocene tonalite sills and Coast shear zone form the western margin of the Central Gneiss Complex. South of Douglas Channel, however, the Coast shear zone and tonalitic sills trace obliquely across axial portions of the Coast Mountains to the eastern margin, progressively truncating the Central Gneiss Complex (Rusmore et al., 2001, 2005).

Paleocene Tonalite Sills

The western margin of the axial portion of the Coast Mountains is characterized by distinctive steeply dipping sills of foliated tonalite that can be traced for tens of kilometers along their northwest-southeast strike, but that are only a few kilometers (locally as much as 10 km) in width (Brew and Ford, 1978; Gehrels et al., 1991; Wheeler and McFeely, 1991). These bodies continue northwestward, apparently continuously, from south of Bella Coola to north of Skagway, a distance of at least 1000 km. Most bodies display a steeply east-dipping foliation and steeply inclined stretching lineation (Ingram and Hutton, 1994; Klepeis et al., 1998; Crawford et al., 1987, 1999, 2000; Rusmore et al., 2001, 2005; Hollister and Andronicos, 2000; Andronicos et al., 2003). The deformation is greatest in westernmost bodies and decreases eastward. Barometric studies, mostly on bodies in southeast Alaska, indicate emplacement depths of ~15–20 km (Hollister et al., 1987; Stowell and Crawford, 2000; Rusmore et al., 2005).

A regional analysis of U-Pb ages (Gehrels et al., 1991) indicates that the tonalitic sills become younger southeastward, from mostly 70 Ma ages in the northwest to mostly 60 and 50 Ma ages in the southeast. There is also a consistent eastward younging of several million years within individual bodies and in successive parallel bodies.

Coast Shear Zone

The Coast shear zone was originally recognized as a topographic and structural lineament, referred to as the Coast Range lineament (Twenhofel and Sainsbury, 1958) or megalineament (Brew and Ford, 1981) in southeast Alaska, and the Work Channel lineament near Prince Rupert (Hutchison, 1982; Crawford et al., 1987). More recent work in the study area has emphasized ductile deformational fabrics that formed early in shear zone history. These ductile fabrics occur within the tonalite sills and in the country rocks between the bodies and along their western margin (Ingram and Hutton, 1994; Klepeis et al., 1998; Klepeis and Crawford, 1999; Rusmore et al., 2001, 2005; Crawford et al., 1999; Andronicos et al., 2003; Hollister and Andronicos, 1997, 2000, 2006). The intensity of deformation is greatest within and along the westernmost tonalitic sill, and it decreases both eastward and westward, such that in most areas, shear zone fabrics are recognized across a width of 5–10 km. Brittle fabrics overprint the ductile fabrics (Davidson et al., 2003); these brittle shear zones tend to control the topographic lineaments recognized by early workers.

Kinematic studies have revealed a complex history of motion; generally, older east-side-up reverse motion (north of Prince Rupert) is overprinted by younger east-side-down extensional motion (Klepeis et al., 1998; Klepeis and Crawford, 1999; Rusmore et al., 2001, 2005; Crawford et al., 1999; Andronicos et al., 1999, 2003; Hollister and Andronicos, 1997, 2000, 2006). The available chronology suggests mainly reverse motion between ca. 65 Ma and ca. 57 Ma followed by normal motion between ca. 57 Ma and ca. 50 Ma. A minimum age of ca. 55–50 Ma on the ductile deformation is indicated by U-Pb ages of crosscutting dikes and by ca. 50 Ma Ar (hornblende and biotite) ages from within and adjacent to the Coast shear zone (Parrish, 1983; Harrison et al., 1979; Rusmore et al., 2001; Andronicos et al., 2003; Hollister and Andronicos, 2006). 30 Ma pseudotachylytes associated with brittle faults have been found near Prince Rupert (Davidson et al., 2003).

Dextral-slip indicators have also been recognized along the Coast shear zone in central southeast Alaska (Stowell and Hooper, 1990) and in the study area (Klepeis et al., 1998; Andronicos et al., 1999, 2003; Hollister and Andronicos, 1997, 2000, 2006). The recognition of dextral slip is consistent with the view that the Coast shear zone formed as part of the southern continuation of the Denali fault (Lanphere, 1978), which has ~370 km of dextral offset (Lowey, 2007). According to this interpretation, the Coast shear zone (and associated structures) would

have accommodated 150–250 km of right-lateral offset, with the remainder of Denali displacement accommodated along the Chatham Strait fault to the west. This model has received significant support from studies in northern southeast Alaska, where the Coast shear zone merges with the Denali fault. In this area, the Coast shear zone is a broad mylonitic zone that records dextral displacement between ca. 63 and ca. 57 Ma (Gehrels, 2000b). As described later, the recognition of dextral slip along the Coast shear zone is also consistent with models that interpret much larger amounts of dextral displacement.

High-Grade Metasedimentary Rocks

A significant proportion of the axial Coast Mountains is underlain by pelitic schist, quartzite, marble, and calc-silicate gneiss, which occur as pendants and screens ranging in size from outcrop to kilometer scale. These rocks are interpreted to belong largely to the Yukon-Tanana terrane (Gehrels et al., 1992; McClelland et al., 1992a; Gareau and Woodsworth, 2000; Gehrels and Boghossian, 2000; Gehrels, 2001), the lower portion of which is equivalent to the Nisling terrane of Wheeler et al. (1991). There may also be components of the Stikine terrane in some areas (Hill, 1985). In most areas, these rocks are sillimanite-bearing, but some localities clearly show that the sillimanite replaces kyanite or staurolite. Petrologic studies, as summarized by Stowell and Crawford (2000), Hollister and Andronicos (2000), and Rusmore et al. (2005), show metamorphism of upper amphibolite to granulite facies.

Orthogneiss and Migmatite

In many regions, the metasedimentary rocks are associated with orthogneiss that has experienced much of the deformation and metamorphism of the metasedimentary assemblages (Crawford et al., 1999; Hollister and Andronicos, 2000; Rusmore et al., 2005). Migmatite is also common.

Granodioritic Plutons and Dike Swarms of Mostly Eocene Age

Granodioritic to granitic bodies, which range from giant plutons to swarms of dikes and sills, intrude the metamorphic assemblages, orthogneiss, and migmatite. In most cases, these bodies are not deformed and intrude across fabrics in the country rocks.

Eastern Coast Mountains Batholith

The eastern portion of the orogen is underlain primarily by Upper Paleozoic through Tertiary sedimentary and volcanic rocks of the Stikine terrane and overlying strata of the Bowser basin, and by plutons that range in age from early Mesozoic to Tertiary (Wheeler and McFeely, 1991; Haggart et al., 2006a, 2006b, 2007; Mahoney et al., 2007a, 2007b, 2007c, 2007d, 2007e, 2009). Plutons of pre–mid-Jurassic age are interpreted to be part of the Stikine terrane because they are presumably related to volcanic sequences (e.g., Hazelton Group) that occur throughout the terrane. Plutons younger than ca. 160 Ma are interpreted to be part of the Coast Mountains batholith because they apparently do not extend eastward into the Stikine terrane.

In contrast to metamorphic assemblages of the Yukon-Tanana terrane in axial and western portions of the batholith, sedimentary, volcanic, and plutonic rocks of the Stikine terrane in the eastern portion are not highly deformed or metamorphosed. Unfortunately, the location, nature, and age of the structures that separate these stratified rocks from the high-grade assemblages are uncertain in much of the study area. Near Kitimat and Terrace, the boundary is an east-dipping normal fault and associated ductile shear zone referred to as the Shames mylonite zone (Heah, 1990, 1991; Andronicos et al., 2003) or eastern boundary detachment (Rusmore et al., 2005). In contrast, near Burke Channel, the boundary is a steeply east-dipping fault that juxtaposes low-grade Stikine strata on the east against amphibolite-facies metasedimentary and metavolcanic rocks of probable Yukon-Tanana affinity on the west. The nature and location of the transition from an east-dipping normal fault near Kitimat to the steep fault near Bella Coola are uncertain.

The eastern portion of the Coast Mountains batholith also differs from the western portion in that mid-Cretaceous compressional structures dip westward and are east-vergent. These thrusts, referred to regionally as the Skeena thrust belt to the north and the eastern Waddington thrust belt to the south, have been mapped along much of the eastern Coast Mountains batholith by Heah (1990, 1991), Rusmore and Woodsworth (1991), Evenchick (1991), and Haggart et al. (2007).

Mid- to Late Tertiary Igneous Rocks

Although most igneous activity in the Coast Mountains ceased at ca. 50 Ma, a large ca. 10 Ma granitic body (Kings Island intrusive suite) and its volcanic cover are exposed between Bella Bella and Bella Coola (Baer, 1973). There are also scattered bimodal mafic/felsic dike and stock complexes and widespread Tertiary mafic dikes.

U-Th-Pb GEOCHRONOLOGIC RESULTS FROM ZIRCON

In total, 313 U-Pb (zircon) and 59 U-Pb (titanite) ages are available from igneous rocks in the study area. Of these, 84 zircon ages and 41 titanite ages are presented herein for the first time. The new age data are presented in detail in Table DR1 and Figures DR4–DR217, whereas the complete set of ages is listed in Table DR2 and shown on Figures DR1–DR3 (see footnote 1).

In the following discussion, the ages are divided into three groups based on the interpretation that this segment of the Coast Mountains batholith consists of three separate magmatic belts: a western magmatic belt that was constructed on the Alexander and Wrangellia terranes prior to 100 Ma; an eastern magmatic belt that was constructed on the Stikine and Yukon-Tanana terranes prior to 110 Ma; and a magmatic belt that was built across the older intrusive units and their host terranes between 100 and ca. 50 Ma. The boundary between the western and eastern magmatic belts is delineated by sedimentary rocks (and their metamorphic equivalents) of the Gravina belt (Figs. 1 and 2A), which record distal marine sedimentation during Late Jurassic–Early Cretaceous time (Berg et al., 1988; Gehrels, 2001). The existence of this basinal sequence between Alexander-Wrangellia and Stikine–Yukon-Tanana precludes continuity of western and eastern portions of the batholith prior to ca. 100 Ma.

The western margin of the Gravina belt is a depositional contact (shown with a green line on Fig. 2A) as mapped near Prince Rupert (Gehrels, 2001) but, to the south, it is intruded by mid- to Late Cretaceous plutons. The eastern margin is a mid-Cretaceous thrust fault that juxtaposes rocks of the Yukon-Tanana terrane over strata of the Gravina belt and underlying Alexander terrane. This fault, shown with a red line on Figure 2A, is preserved near Prince Rupert (Gehrels, 2001) but is everywhere intruded by mid- to Late Cretaceous plutons to the south. The location to the south of both boundaries is accordingly bracketed between pendants of contrasting tectonic affinity and the occurrence of metamorphosed Gravina strata in a narrow belt between Bella Coola and Bella Bella (Fig. 2A).

All of the U-Pb ages younger than 230 Ma from the study area are projected onto an east-west profile on Figure 6. Because of the uncertainty in location of the boundary between eastern and western belts, the position of the samples is shown relative to

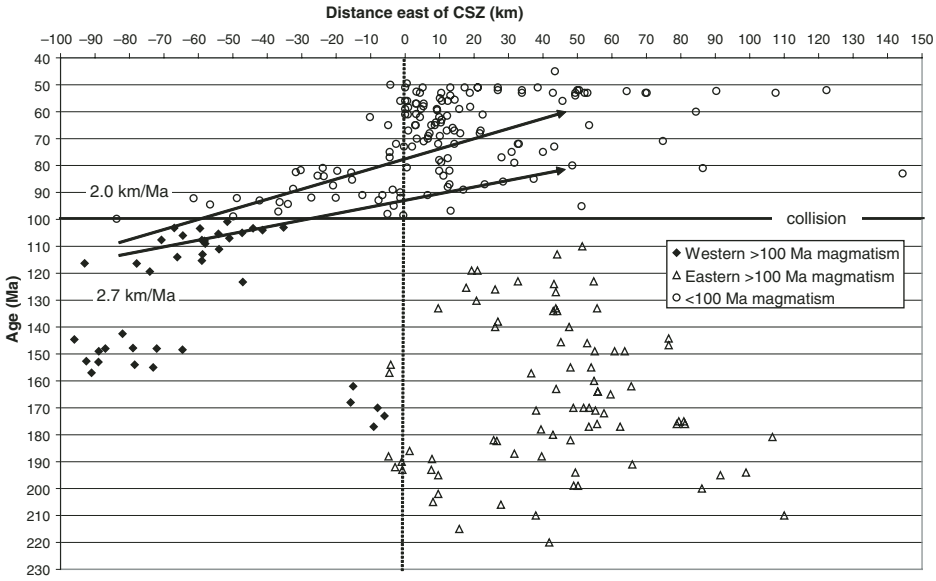

Figure 6. Plot of U-Pb (zircon) ages projected onto a northeast-southwest transect, referenced to distance from the Coast shear zone (CSZ). Onset of collision at 100 Ma is interpreted from geologic relations described in the text. Migration rates are shown for least-squares fit through all 120–80 Ma and 120–60 Ma ages.

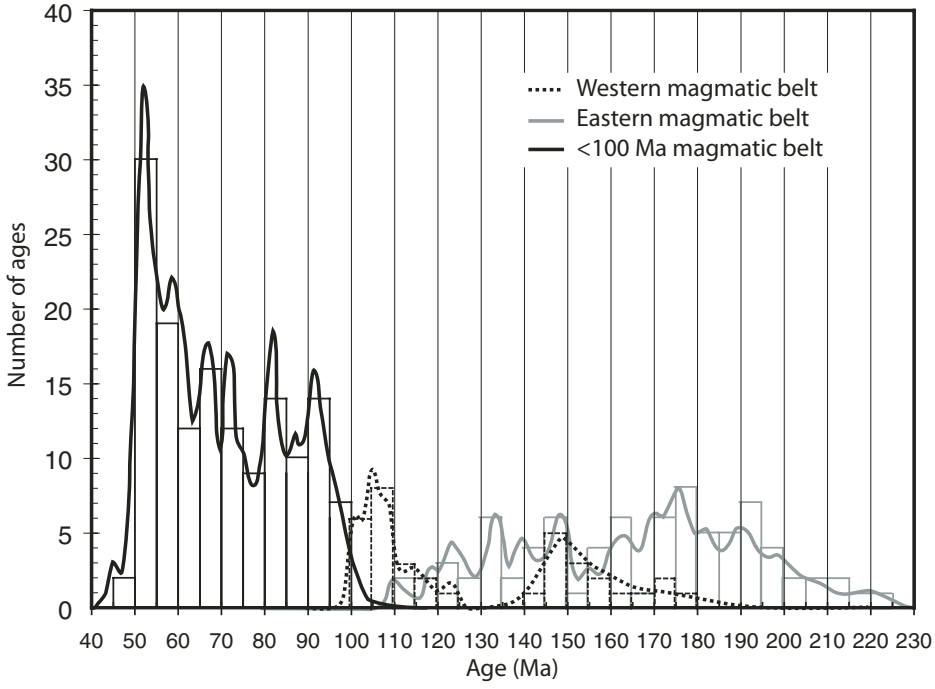

Figure 7. Relative age-distribution plot of U-Pb (zircon) ages divided into western, eastern, and younger than 100 Ma belts. Note that the curves are not normalized for either the number of analyses or the magmatic flux.

the western margin of the Coast shear zone, which can be mapped throughout the study area with confidence. Ages from the three belts are also plotted on a set of histograms and age-distribution diagrams (Fig. 7).

Western Magmatic Belt

Seventeen new U-Pb (zircon) ages were determined on pre–100 Ma plutonic samples that intrude rocks of the Alexander and Wrangellia terranes. These ages, together with 22 ages reported by Butler et al. (2006), Crawford et al. (2009), Friedman and Mortensen (2002), Gehrels and Boghossian (2000), Gehrels (2001), Saleeby (2000), and van der Heyden (1989, 1992), define three apparent clusters of magmatism (Figs. 6 and 7). Oldest are ages of 177–162 Ma (maximum age probability of 169 Ma), primarily on volcanic rocks that occur along the inboard margin of the Alexander terrane. This magmatism appears to have ceased at ca. 160 Ma, with a second phase of magmatism occurring on the outermost islands from 157 to 142 Ma (maximum age probability at 149 Ma). Magmatism appears to have ceased between ca. 140 and ca. 120 Ma, with only one dioritic body emplaced at ca. 123 Ma. The third phase of magmatism initiated at 118 Ma and continued through 100 Ma. The maximum age probability for this set of ages is at 106 Ma.

Eastern Magmatic Belt

Seventeen new U-Pb (zircon) ages were determined on pre–110 Ma plutonic samples that intrude rocks of the Stikine and Yukon-Tanana terranes. These samples, together with 65 samples from Gareau (1991a), Saleeby (2000), van der Heyden (1989, 1992, 2004), Gehrels and Boghossian (2000), Gehrels (2001), Haggart et al. (2006a, 2006b, 2007), Diakow (2006), and Mahoney et al. (2007a, 2007b, 2007c, 2007d, 2007e, 2009), yield ages that range from ca. 225 to ca. 110 Ma. As shown on Figure 7, magmatism was apparently continuous through this time, since there are no significant age-distribution peaks or gaps.

Younger than 100 Magmatic Belt

In total, 146 U-Pb (zircon) ages younger than 100 Ma are available from the study area, of which 47 are reported herein. These igneous bodies intrude rocks of the Alexander-Wrangellia and Stikine–Yukon-Tanana terranes, and rocks of the Gravina belt between them, and they are accordingly interpreted to postdate juxtaposition of the two crustal fragments and their magmatic belts. Onset of this magmatism occurred at 100 Ma, and it appears to have been continuous with magmatism in the western belt (Fig. 6). In contrast, magmatism in the eastern belt ceased at ca. 110 Ma, and there was a lull of ~20 Ma before magmatism resumed in eastern regions at ca. 90 Ma (Mahoney et al., 2009) (Fig. 6).

Magmatism in this time period appears to have migrated eastward, with most 90–80 Ma magmatism west of the Coast shear zone, most 80–60 Ma magmatism in axial portions of the

Coast Mountains, and 60–50 Ma magmatism occurring from the Coast shear zone eastward for a considerable (>150 km) distance.

MIGRATION OF MAGMATISM

Migration of magmatism clearly occurred in western and axial portions of the batholith, but it is not apparent to the east (Fig. 6). The most obvious pattern of migration is recorded by the eastward younging of plutons ranging from 120 to 80 Ma and perhaps 60 Ma. This was first observed by van der Heyden (1989, 1992), and it is confirmed by the results of our study. A regression of all 120–80 Ma ages yields a migration rate of 2.7 km/Ma (R^2 = 0.51), whereas a regression through 120–60 Ma ages yields a rate of 2.0 km/Ma (R^2 = 0.46). In the southern Coast Mountains batholith, south of our study area, plutons of 120–80 Ma also young eastward, with a migration rate of 2.0 km/Ma (R^2 = 0.31) (Friedman and Armstrong, 1995). These rates are similar to a migration rate of 2.7 km/Ma reported for 120–80 Ma plutons in the Sierra Nevada batholith (Chen and Moore, 1982).

MAGMATIC FLUX

We have attempted to reconstruct the magmatic flux for this portion of the Coast Mountains batholith by (1) dividing the batholith into panels that appear homogeneous in terms of the proportions of plutonic rocks of various ages (Fig. 8), (2) reducing the area of each panel by the percent of nonplutonic rocks exposed, based on geologic maps of the region (Table 1), (3) multiplying the areal exposure of plutonic rocks in each panel by a paleodepth of 25 km (following Ducea and Barton's [2007] analysis of the Sierra Nevada batholith) to get an approximate volume of igneous rocks, (4) dividing by the northwest-southeast length of each panel to get the volume per kilometer of strike length, and (5) dividing the resulting value by the duration of magmatism in each panel. Because western and eastern portions of the batholith were not contiguous prior to ca. 100 Ma, their magmatic fluxes were calculated separately (Table 1).

Igneous bodies younger than Eocene were omitted from this calculation; these include mafic dikes that are widespread in the study area, a young (ca. 10 Ma) granite body located near Bella Bella, and scattered Tertiary volcanic rocks (Wheeler and McFeely, 1991). Represented with considerable uncertainty are migmatitic rocks in the Central Gneiss Complex (axial portion of the batholith). These rocks are generally interpreted to be early Tertiary in age based on proximity to plutons and dikes of known Paleocene-Eocene age, but this has not been confirmed geochronologically. It is also difficult to determine the volumetric contribution of migmatitic rocks given that their distribution is highly variable. As a first approximation, we have included these migmatitic rocks as Paleocene-Eocene in age and comprising 25% (distributed as 5% at 64–55 Ma and 20% at 55–48 Ma) of the Central Gneiss Complex (Table 1).

This analysis yields an estimate of the magmatic flux through time, expressed in cubic

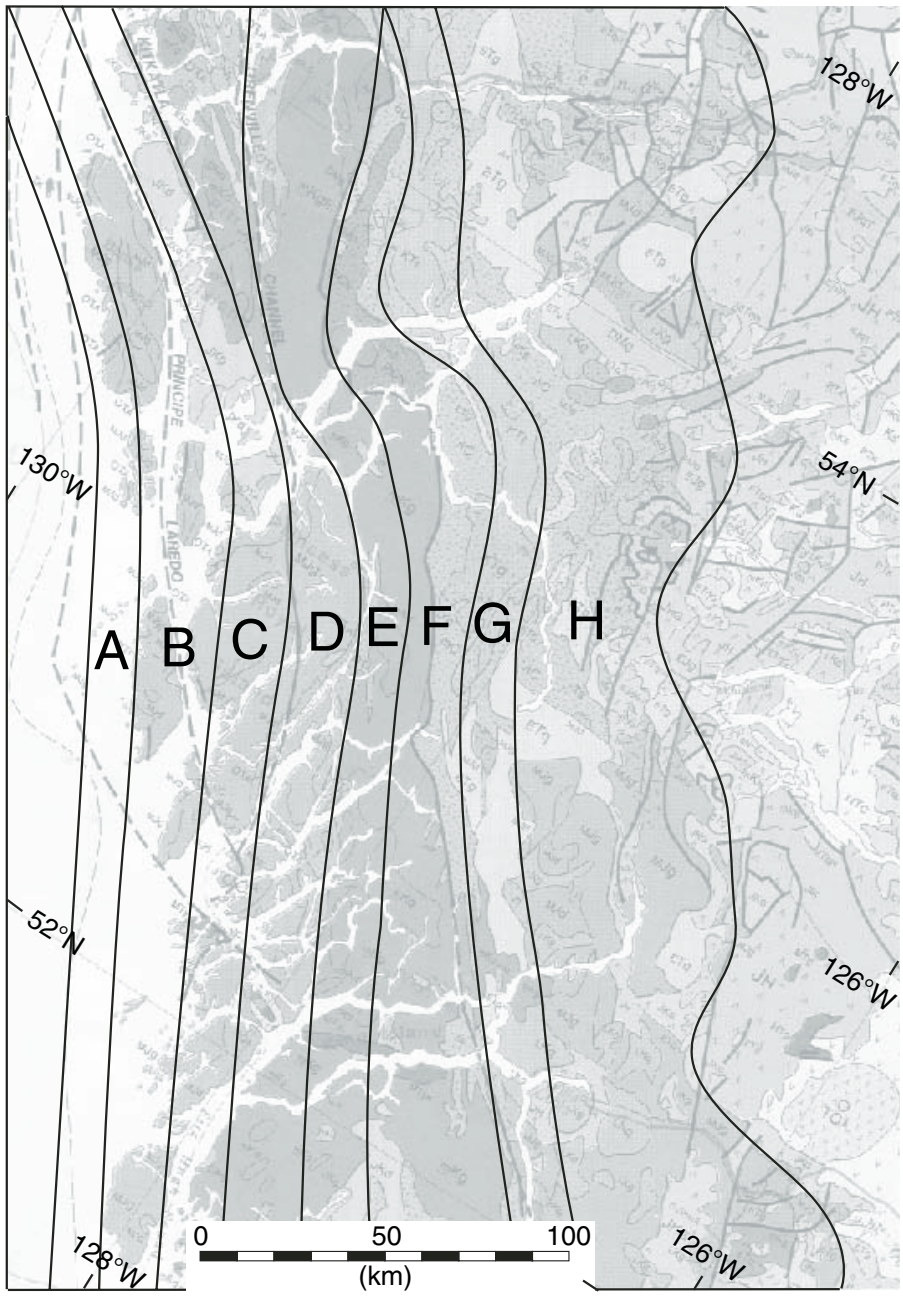

Figure 8. Division of study area into panels used for determination of magmatic flux (see the Appendix for definition of map units). The volume of plutonic rock in each panel was determined by subtracting the proportion of nonplutonic rock shown on the geologic map of Wheeler and McFeely (1991) (Table 1), and assuming that the plutonic rocks originally had a vertical extent of 25 km (from Ducea and Barton, 2007). For panels that contain multiple ages of plutons, e.g., G and H, the volumes apportioned to each age range were determined from the map distribution shown by Wheeler and McFeely (1991).

TABLE 1A. CALCULATION OF AVERAGE MAGMATIC FLUX FOR DIFFERENT PORTIONS OF THE COAST MOUNTAINS BATHOLITH (CMB) IN THE STUDY AREA (PERCENT OF PLUTONIC ROCK OF EACH AGE INTERVAL; KEYED TO FIGURE 8 PANELS)

Age range (Ma)	A (%)	B (%)	C (%)	D (%)	E (%)	F (%)	G (%)	H (%)
55–48							10	21*
64–55							40	5§
78–64							30	7†
89–78						70	10	3§
99–89					85			3†
110–99				85				0†
121–110			90					16†
130–121								2§
140–130								7†
152–140		90						0†
160–152	90							1§
167–160								1§
185–167								1†
225–185								3†
Other	10	10	10	15	15	30	10	30

*Estimated from distribution of Eocene plutons shown by Wheeler and McFeely (1991), with an additional 20% of Central Gneiss Complex (which occupies 16% of the area of panel H) for 55–48 Ma migmatites.

†Estimated from distribution of plutonic suites in Mahoney et al. (2009) study area.

§Estimated from number of ages present in panel H plus 5% of Central Gneiss Complex for 64–55 Ma migmatites.

TABLE 1B. AVERAGE MAGMATIC FLUX FOR EACH AGE INTERVAL IN EACH PANEL (KEYED TO FIGURE 8 PANELS)

Age range (Ma)	A	B	C	D	E	F	G	H	TOTAL
55–48							5.5	43.1	48.6
64–55							17.2	8.0	25.2
78–64							8.3	7.2	15.5
89–78						36.1	3.5	3.9	43.5
99–89					40.3			4.3	44.6
110–99				35.0				0	
121–110			31.8					20.9	
130–121								2.6	
140–130								10.0	
152–140		37.1						0	
160–152	32.9							1.2	
167–160								2.1	
185–167								0.8	
225–185								1.1	

Note: Magmatic flux is calculated as area × % plutonic rock × 25 km (depth)/strike length of panel/duration of age interval, resulting in units of km^3/Ma per km of strike length.

kilometers per million years per kilometer of strike length, for the western and younger than 100 Ma portions of the batholith (histogram bars on Fig. 9). These average magmatic flux values were then converted into an interpreted magmatic flux curve (solid line on Fig. 9) by assuming that a more accurate magmatic flux during each time period is represented by the age-distribution curve (dashed line, from Fig. 7).

Although the assumptions inherent in this analysis (e.g., that we have accurately determined the proportion and original vertical extent of igneous rock in each panel, and that our sample suite represents all volumetrically important igneous components) result in considerable uncertainty in both the absolute and relative magnitudes of the high-flux episodes, there is little doubt that the magmatic flux in the western and central portions of the batholith was strongly episodic. Magmatic flux values for the eastern portion of the batholith are less well constrained, but they clearly are much lower (Table 1).

It should also be noted that these calculations systematically underestimate the total magmatic flux of the batholith because volcanic equivalents of the plutonic rocks are not included. Assuming a typical plutonic:volcanic ratio of 3:1–5:1 (de Silva and Gosnold, 2007; Ducea and Barton, 2007), actual magmatic flux values are probably higher by a factor of 1.2–1.33.

Our magmatic flux analysis suggests that this portion of the Coast Mountains batholith experienced three distinct flare-up events at 160–140 Ma (~35 km^3/Ma per km strike length), 120–78 Ma (35–45 km^3/Ma per km

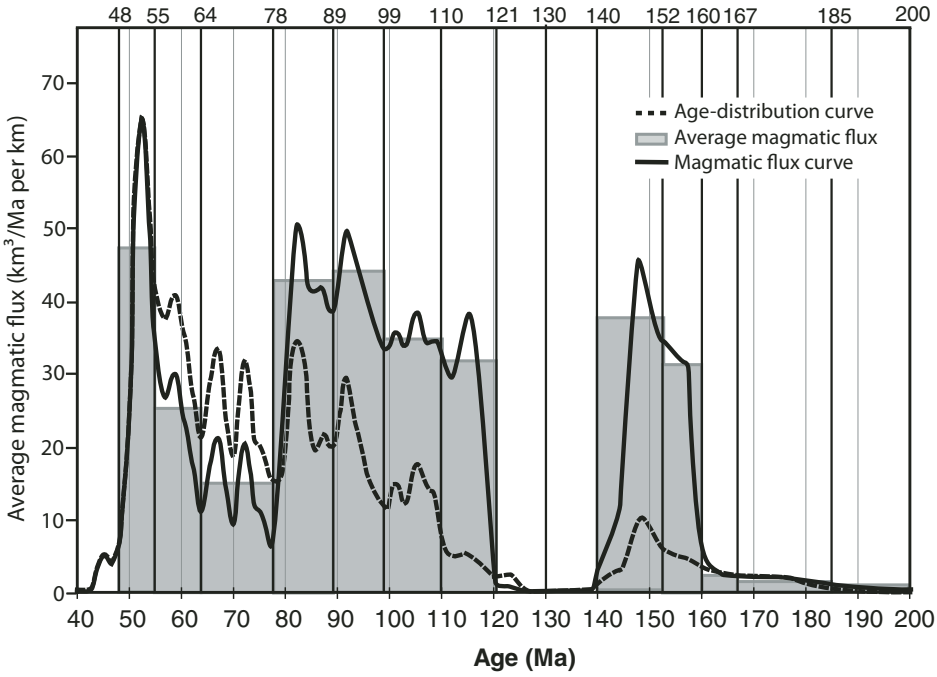

Figure 9. Plot showing the magmatic flux interpreted for the western and younger than 100 Ma magmatic belts. The average magmatic flux for each age interval (from Fig. 2B) was determined by calculating the volume of plutonic rock in each panel (Fig. 8), apportioning this volume according to the different age groups present in each panel, and dividing by the strike length of each panel and the age duration of each magmatic interval (Table 1). This yielded an average magmatic flux for each age interval, expressed in km^3/Ma per km strike length (vertical bars). The actual magmatic flux through time (solid curve) is interpreted to be represented by the age distribution of the western and younger than 100 Ma magmatic belts (dashed curve, from Fig. 7), adjusted such that the curve for each age interval occupies the same volume as the average flux.

strike length), and 55–48 Ma (~50 km^3/Ma per km strike length) (flux values do not include volcanic equivalents; Table 1; Fig. 9). Magmatic lulls are recorded at 140–120 Ma and 78–55 Ma. The interpreted tectonic setting during each of these phases is described later.

U/Th CONSTRAINTS ON METAMORPHISM

U/Th values provide a powerful tool for determining whether metamorphic fluids were present when zircon grains crystallized (or recrystallized) (Williams, 2001; Rubatto, 2002; Rubatto et al., 2001; Hoskin and Schaltegger, 2003), although Harley et al. (2007) pointed out that high U/Th values can also occur in igneous systems. In most cases, zircons that crystallized in the presence of metamorphic fluids have high U/Th (>10–20) and high U concentration (>1000–2000 ppm) due to the enrichment of U in fluid-rich environments, exclusion of Th during zircon recrystallization, and regional depletion of Th during growth of metamorphic monazite.

Figure 10 is a plot of U/Th for the 2182 zircons analyzed by LA-ICP-MS that yield ages between 40 Ma and 220 Ma. Each symbol represents the measured U/Th for a single spot analysis, plotted according to the measured $^{206}Pb/^{238}U$ age. Diamonds represent measurements on crystals with no discernible age zonation, whereas squares and triangles are from cores and rims (respectively) of crystals that are zoned in age. The solid curve, calculated by summing the U/Th values for each age, provides a graphic measure of U/Th patterns through time.

Excursions toward high U/Th values indicate that metamorphic zircon crystallized (or recrystallized) at ca. 88–76 Ma and ca. 62–52 Ma. A comparison with the magmatic flux curve (dashed line) indicates that the growth/recrystallization of metamorphic zircon coincides with two of the main phases of high magmatic flux. Tectonically, these phases of high flux magmatism and metamorphic zircon growth/recrystallization coincide with significant Late Cretaceous crustal thickening and regional metamorphism in western and central portions of the batholith, and with early Tertiary crustal extension in central and eastern portions of the batholith.

U-Th-Pb GEOCHRONOLOGIC RESULTS FROM TITANITE

U-Pb geochronologic data on titanite were gathered from 41 samples, most of which also yielded zircon ages (described already). Eighteen additional titanite ages have been reported previously by Klepeis and Crawford (1999), Crawford et al. (1999, 2009), Andronicos et al. (2003), Friedman et al. (2001), and Rusmore et al. (2005). These ages range from ca. 196 Ma to ca. 49 Ma; younger ages occur in axial portions of the Coast Mountains, and older ages occur to both the east and west (Fig. 3).

Figure 11 shows the titanite ages plotted versus east-west position, where the ages have been divided into samples that occur west of the Coast shear zone, samples that occur east of the Shames mylonite zone–eastern boundary fault, and samples that occur between the Coast shear zone and the Shames mylonite zone–eastern boundary fault. The ages of zircons from the same samples, where available, are also shown on Figure 11. In the west, the zircon and titanite ages are generally similar, reflecting the relatively shallow level of emplacement of these plutons and the lack of younger thermal overprinting (Butler et al., 2006). East of the Coast shear zone, the titanite ages are mainly between 60 and 50 Ma, whereas most zircon ages from the same samples are considerably older. This young cooling reflects rapid exhumation of axial portions of the batholith during early Tertiary time (Hollister, 1982; Crawford et al., 1987; Andronicos et al., 2003; Rusmore et al., 2005) combined with thermal resetting during emplacement of widespread ca. 55–50 Ma plutons and dikes.

Early Tertiary exhumation and cooling of axial portions of the Coast Mountains batholith are interpreted to have occurred in an extensional regime (Gehrels and McClelland,

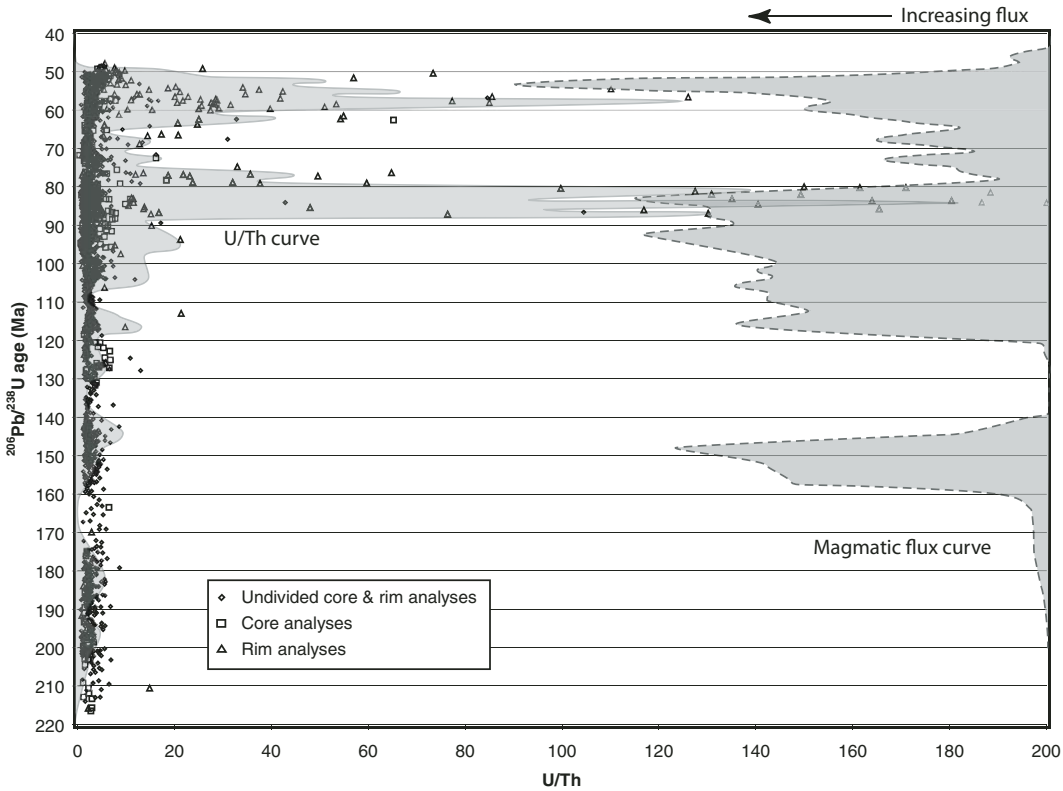

Figure 10. U/Th values for zircon analyses (n = 2182) conducted by laser-ablation–multicollector–inductively coupled plasma–mass spectrometry (LA-MC-ICP-MS) (from Table DR1 [see text footnote 1]; Rusmore et al., 2005). The U/Th curve (solid line), which is simply the sum of these U/Th values, offers a graphic representation of U/Th through time. The interpreted magmatic flux (dashed line, with increasing values to the left) is shown for comparison. See text for discussion.

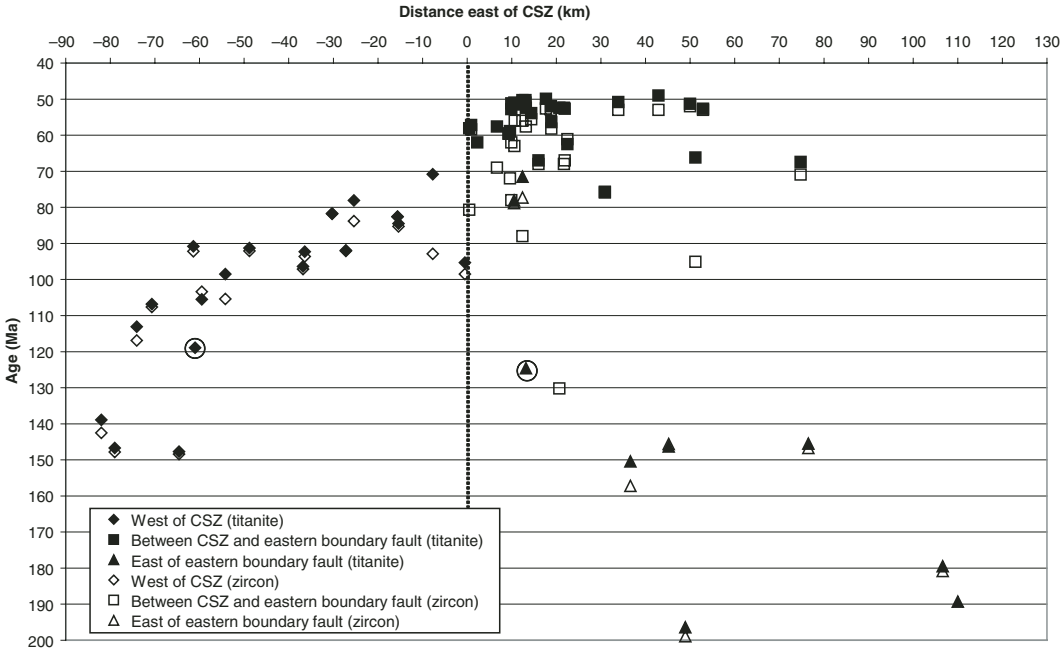

Figure 11. Plot of U-Pb (titanite) ages projected onto a northeast-southwest transect, referenced to distance from the Coast shear zone (CSZ). Solid symbols are for titanite ages, and open symbols show zircon ages from the same sample (where available). Titanite ages that lack zircon ages are encircled. The difference between zircon and titanite ages in axial portions of the batholith, and the clustering of titanite ages between 60 and 50 Ma, provides evidence of rapid uplift and cooling of axial portions of the batholith during early Tertiary time.

1988), with normal motion along the northern Coast shear zone and the Shames mylonite zone (Heah, 1990, 1991; Cook and Crawford, 1994; Klepeis et al., 1998; Klepeis and Crawford, 1999; Crawford et al., 1999; Rusmore et al., 2001, 2005; Andronicos et al., 1999, 2003; Hollister and Andronicos, 2000, 2006).

TECTONIC SYNTHESIS

Magmatism within the Coast Mountains batholith clearly formed in a convergent margin setting, and this batholith shares many similarities with the Peninsular Ranges, Sierra Nevada, and Idaho batholiths. Since at least mid-Cretaceous time, these batholiths record the subduction of paleo-Pacific oceanic plates along the western margin of the North American continent (Engebretson et al., 1985).

Most workers agree that the Coast Mountains batholith evolved as a single west-facing magmatic arc from mid-Cretaceous through early Tertiary time. As described initially by Crawford et al. (1987), mid- and Late Cretaceous magmatism occurred in a compressional regime during underthrusting of the Alexander-Wrangellia terrane beneath the western margin of the Stikine and Yukon-Tanana terranes. An alternative view, referred to as the Baja British Columbia hypothesis, uses paleomagnetic data to argue that the western portion of the Coast Mountains batholith was located ~1500–2000 km south of its present position (relative to the eastern part of the batholith, and to North America), as recently as ca. 70 Ma (Cowan et al., 1997; Hollister and Andronicos, 1997; Miller et al., 2006). The Coast shear zone is viewed as a possible locus of much of this displacement. As summarized by Butler et al. (2001b), however, an alternative explanation of the available paleomagnetic data, involving tilting of plutons and compaction shallowing of clastic strata, is consistent with the existence of a single Late Cretaceous–early Tertiary arc.

There is also disagreement about the number and polarity of magmatic arcs prior to mid-Cretaceous time. The simplest tectonic model is that of Armstrong (1988) and van der Heyden (1989, 1992), in which the Coast Mountains batholith represents a single, long-lived, west-facing magmatic arc. According to this model, west-facing subduction occurred continuously along the western Canadian margin from Middle Jurassic through early Tertiary time. The Gravina and Tyaughton-Methow Basins are interpreted to have opened as backarc basins, pulling the outboard arc away from the continental margin, and then closed during mid-Cretaceous time. McClelland et al. (1992b) revised this model by having the Gravina and Tyaughton-Methow Basins form in a regime of dextral transtension as the outboard arc (and its Alexander-Wrangellia underpinnings) moved northward along the Cordilleran margin.

Monger et al. (1982) proposed an alternative model in which the western arc and underlying Alexander-Wrangellia basement were separated from the eastern arc and Stikine–Yukon-Tanana basement by a broad ocean basin. This basin closed by east-dipping subduction beneath the eastern arc, trapping the Gravina belt as a backarc basin and the Tyaughton-Methow as a forearc basin along the collisional suture. Mid-Cretaceous through early Tertiary magmatism is interpreted to have occurred at least in part due to crustal melting generated by collisional processes.

A third possibility, presented by Monger et al. (1994), is that the western portion of the batholith was the northern continuation of the eastern part of the batholith during Late Jurassic–Early Cretaceous time, and that these two magmatic belts were subsequently juxtaposed by sinistral translation of the northern portion of the arc to a position outboard of the southern portion of the arc. In this model, the Gravina belt formed as a backarc basin behind the northern/western arc, whereas the Tyaughton-Methow Basin formed in a forearc position relative to the southern/eastern arc system. Approximately 800 km of sinistral motion is interpreted to have occurred along a fault system that cut obliquely across the convergent margin system (Monger et al., 1994).

The latter model is interpreted to be the most likely explanation of the Late Jurassic–Early Cretaceous setting of the Coast Mountains batholith because it is consistent with tectonic relations farther north along the Cordilleran margin (e.g., Ridgway et al., 2002), and it offers a reasonable explanation of many of the first-order constraints in the study area, as follows:

(1) The western and eastern magmatic belts are similar in that both record magmatism from ca. 160 to ca. 100 Ma and both were apparently west-facing (although there are significant differences in their magmatic histories; Fig. 7).

(2) The eastern magmatic belt, which continues southward along the Cordilleran margin to at least northern Mexico, does not extend north of Terrace, whereas the western magmatic belt continues northward along the margin to mainland Alaska but does not continue south of Vancouver and Victoria (Fig. 12).

(3) The Gravina belt appears to have formed in a backarc position, whereas the Tyaughton-Methow Basin clearly formed in a forearc position (Monger et al., 1994; DeGraaff-Surpless et al., 2003).

(4) There are subduction complexes of Middle Jurassic through Early Cretaceous age (Monger et al., 1994) associated with Tyaughton-Methow basinal strata. These can be traced northward into the southern Coast Mountains, outboard of the eastern magmatic belt, but subduction complexes have not been recognized along the suture zone to the north.

(5) Sinistral displacement is consistent with rapid northwestward absolute motion of North America during Late Jurassic–Early Cretaceous time and a sinistral component of North America–Farallon convergence (Engebretson et al., 1985).

Next, we provide a series of paleotectonic reconstructions that frame our preferred interpretation for the magmatic evolution of the central Coast Mountains batholith (Fig. 12). Critical aspects of each reconstruction are as follows:

(1) Ca. 155 Ma (Late Jurassic; Fig. 12A). Following mid-Jurassic juxtaposition of Alexander-Wrangellia against the outboard margin of Stikine and Yukon-Tanana (McClelland et al., 1992a; Saleeby, 2000), the western portion of the batholith is interpreted to have formed as the northern continuation of the eastern portion of the batholith. The Gravina belt opened in a backarc position relative to the northern/western magmatic arc, whereas the Tyaughton-Methow Basin developed in a forearc position relative to the southern/eastern magmatic arc. Various Jurassic-Cretaceous subduction complexes in and adjacent to the southern Coast Mountains (e.g., Bridge River, Hozameen, Shuksan, and Cayoosh assemblages) record subduction along this convergent margin. Similar assemblages are inferred to have continued northward outboard of the western arc, and they may be represented by older portions of the Chugach terrane.

High-flux magmatism in the western portion of the batholith between 160 and 140 Ma occurred during regional crustal extension that formed the Gravina basin, following mid-Jurassic compression and prior to the onset of mid-Cretaceous tectonism. It is unclear whether this 160–140 Ma magmatic arc was stationary or migrated eastward (Fig. 6).

(2) Ca. 120 Ma (Early to mid-Cretaceous; Fig. 12B). Beginning in Early Cretaceous time, the northern/western magmatic belt is interpreted to have moved southward along a sinistral fault system that cut obliquely across the convergent margin. Sinistral motion is documented along the Kitkatla fault and other shear zones along the west flank of the Coast Mountains at ca. 110 Ma (Chardon et al., 1999; Chardon, 2003; Butler et al., 2006), but motion may have commenced earlier in Cretaceous time. Sinistral motion during this time frame is also recorded in the eastern portion of the batholith (Mahoney et al., 2009). Approximately 800 km of sinistral displacement is required to provide the present overlap of the western and eastern magmatic belts, but southward displacement could have been considerably greater.

Sinistral motion along such a fault system may also explain the occurrence of the long belt of Yukon-Tanana terrane along the western margin of the Stikine terrane. In this view, an alternative to the oroclinal rotation model of Mihalynuk et al. (1994), rocks of the Yukon-Tanana terrane in the Coast Mountains would have formed as a western continuation of the large expanse of Yukon-Tanana terrane in Yukon and eastern Alaska, and then moved southward outboard of the Stikine terrane.

In the western belt, magmatic flux was quite low between 140 and 120 Ma (Fig. 9), perhaps in response to an oblique sinistral component of plate convergence (Engebretson et al., 1985). In the eastern arc, magmatism terminated at ca. 110 Ma as Alexander-Wrangellia and the western arc moved southward and progressively shielded this region from subduction. Unfortunately, our data set does not have the resolution to determine whether cessation of magmatism migrated southward, as would be expected in this model.

Following the 140–120 Ma magmatic lull in the western belt, high-flux magmatism initiated within and immediately east of the belt of 160–140 Ma plutons (Fig. 2A), and then it began to migrate eastward at ~2 km/m.y. Eastward migration continued into Late Cretaceous and possibly early Tertiary time, following a pattern that is also recorded in the southern Coast Mountains batholith (Friedman and Armstrong, 1995) and the Sierra Nevada batholith (Chen and Moore, 1982). The continued accumulation of distal marine strata within the Gravina belt suggests that early stages of this high-flux magmatism, between 120 and 100 Ma, occurred in a regime of overall extension or sinistral transtension.

(3) Ca. 85 Ma (Late Cretaceous; Fig. 12C). During mid-Cretaceous time, the Gravina belt and Tyaughton-Methow Basins collapsed, and the Alexander-Wrangellia terrane was accreted to the western margin of the Stikine and Yukon-Tanana terranes (Fig. 12C), juxtaposing the northern/western and southern/eastern magmatic assemblages. High-flux magmatism continued to migrate eastward during this accretionary event, and 100–80 Ma magmatism occurred continuously across the suture zone, effectively welding the older magmatic arcs, and their host terranes, together. High-flux magmatism after ca. 100 Ma accordingly occurred in a compressional regime during formation of a west-vergent thrust belt along the west flank of the orogen, an east-vergent thrust belt along the eastern margin of the orogen, and an early phase of east-side-up reverse motion along the Coast shear zone. Regional metamorphism and growth/recrystallization of metamorphic zircon occurred during this phase of high-flux magmatism.

Late Cretaceous–early Tertiary magmatism is interpreted to have occurred within a regime of overall dextral transpression (e.g., Hollister and Andronicos, 2006). Dextral motion was localized along major faults inboard of the Coast Mountains (Gabrielse et al., 2006; Wyld et al., 2006), and also faults such as the Yalakom, Harrison Lake, and related faults that project into the southern Coast Mountains. Dextral slip also occurred on faults outboard of the Coast Mountains batholith, such as the Denali fault system, Chatham Strait fault, and Clarence Strait fault. As suggested by Lanphere (1978), the Coast shear zone may have transferred ~150–250 km of dextral slip from the Denali fault southward onto the Yalakom, Harrison Lake, and related faults (Wyld et al., 2006). Total dextral displacement may have totaled ~200 km to as much as ~2000 km (according to the Baja British Columbia hypothesis), which would require an equivalent amount of >800 km sinistral displacement during Early Cretaceous time.

The transition from mid-Cretaceous compressional tectonism to Late Cretaceous–early Tertiary dextral transpression appears to have coincided with a dramatic reduction in magmatic flux at ca. 78 Ma, which continued until ca. 55 Ma (Fig. 9). This magmatic lull was presumably related to obliquity of plate convergence along the continental margin, although relative proportions of dextral versus orthogonal convergence are unknown due to uncertainties in plate configuration and hotspot motion (Engebretson et al., 1985; Haeussler et al., 2003; Tarduno et al., 2003).

(4) Ca. 55 Ma (Eocene; Fig. 12D). Eocene high-flux magmatism and growth/recrystallization of metamorphic zircon is interpreted to have occurred within an extensional regime, with east-side-down motion along the northern Coast shear zone and the Shames mylonite zone–eastern boundary fault (Fig. 12D). This extensional tectonism occurred within axial portions

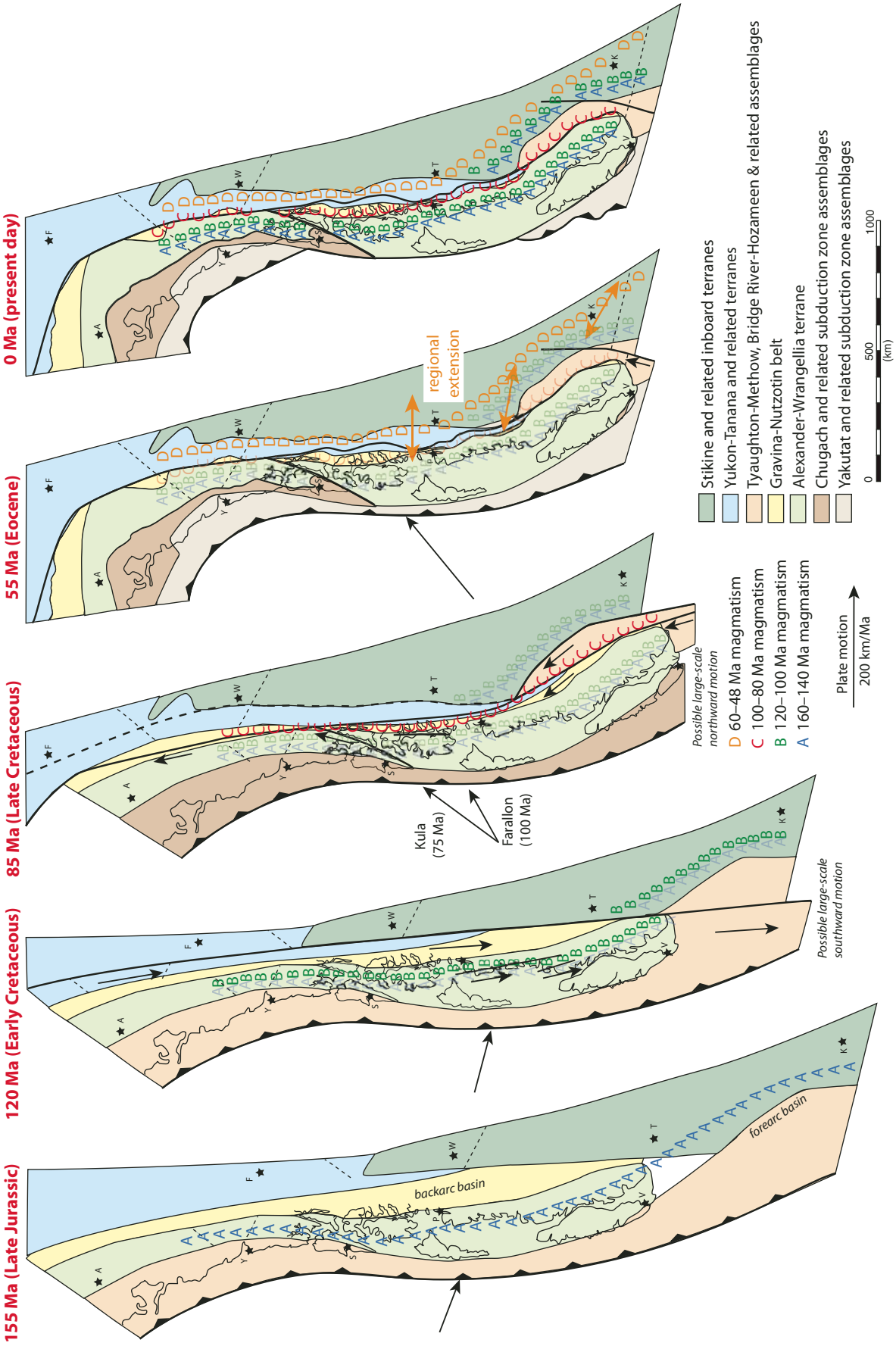

Figure 12. Schematic model offered for the tectonic evolution of the southern Coast Mountains batholith. Plate motion vectors are from Engebretson et al. (1985). See text for discussion.

of the northern and central Coast Mountains, but the evidence is now located east of the Coast Mountains south of Terrace. It is likely that this extensional tectonism is the northern continuation of core complex development in southeastern British Columbia and the northwestern United States. Rapid exhumation of axial portions of the northern and central Coast Mountains batholith occurred during Eocene time in response to this extensional tectonism.

High-flux magmatism at ca. 55–48 Ma and rapid exhumation of axial portions of the Coast Mountains batholith were interpreted by Haeussler et al. (2003) to result from subduction of young and buoyant oceanic lithosphere of the Resurrection plate. Cessation of Coast Mountains batholith magmatism at 50–48 Ma may have resulted from complete removal of the Resurrection plate.

SUMMARY AND CONCLUSIONS

The Coast Mountains batholith provides an excellent laboratory in which to examine the genetic relations among magmatism, metamorphism, uplift, terrane accretion, and plate interactions. The large number of U-Pb ages from igneous rocks demonstrates that the batholith was active nearly continuously from ca. 170 Ma to ca. 50 Ma, but that there were dramatic variations in magmatic flux during this time. The patterns of magmatism also demonstrate that the batholith consists of two pre–mid-Cretaceous magmatic entities that have been juxtaposed by translational and accretionary motion. First-order findings from our study are as follows:

(1) The western portion of the Coast Mountains batholith records magmatism at 177–162 Ma (maximum age probability of 169 Ma), 157–142 Ma (maximum age probabilities at 154 and 149 Ma), and 118–100 Ma (maximum age probability at 108 Ma), with a magmatic lull from 142 to 123–118 Ma (Figs. 6 and 7).

(2) The eastern portion of the batholith records similar overall timing, except that magmatism was apparently continuous between ca. 140 and ca. 120 Ma and ceased at ca. 110 Ma (Figs. 6 and 7).

(3) Magmatism in axial portions of the batholith ranged from ca. 100 to ca. 50 Ma, and plutons were emplaced into the Alexander and Wrangellia terranes to the west, the Yukon-Tanana and Stikine terranes to the east, and the Gravina belt and mid-Cretaceous thrust faults that separate inboard and outboard terranes (Fig. 6).

(4) Magmatism migrated eastward from 120 Ma to ca. 80 Ma, and possibly to ca. 60 Ma, at a rate of ~2.0–2.7 km/Ma (Fig. 6). This timing and migration rate are very similar to that recorded in the southern Coast Mountains batholith (Friedman and Armstrong, 1995) and the Sierra Nevada batholith (Chen and Moore, 1982).

(5) Measured U/Th values indicate that widespread growth/recrystallization of metamorphic zircon occurred in axial regions of the Coast Mountains batholith during Late Cretaceous thrusting and regional metamorphism (between 88 and 76 Ma, peak at 84 Ma) and during the onset of early Tertiary crustal extension (between 62 and 52 Ma, peak at 58 Ma).

(6) Magmatic flux values for the western and younger than 100 Ma portions of the Coast Mountains batholith record three flare-ups at 160–140 Ma, 120–78 Ma, and 55–48 Ma, with magmatic lulls at 140–120 Ma and 76–55 Ma (Fig. 9). Flux values during the flare-ups ranged between 35 and 50 km^3/Ma per km strike length (not including volcanic equivalents). Late Cretaceous crustal thickening played a significant role in generating the high-flux magmatism between 100 and 78 Ma, whereas high-flux magmatism at 160–140 Ma, 120–100 Ma, and 55–48 Ma apparently occurred during regional crustal extension. An additional difference in magmatic history is that high-flux magmatism between 120 and 78 Ma occurred while the locus of igneous activity migrated eastward (at ~2.0–2.7 km/Ma), whereas magmatism during older (160–140 Ma) and younger (55–48 Ma) high-flux periods was apparently static.

(7) U-Pb ages of titanite, together with previously published Ar ages, demonstrate that the axial portion of the batholith in the northern part of the study area was exhumed and cooled rapidly during Eocene time, ca. 55–48 Ma. This exhumation was associated with east-side-down normal slip on the northern Coast shear zone and the Shames mylonite zone–eastern boundary fault.

(8) The history of magmatism, metamorphism, deformation, and uplift in this portion of the Coast Mountains batholith, combined with regional constraints, is interpreted to be most consistent with the following tectonic model (Fig. 12).

The western portion of the batholith is interpreted to have formed as a northern continuation of the eastern portion of the batholith during Late Jurassic–Early Cretaceous time, with high-flux magmatism at 160–140 Ma in a regime of regional crustal extension.

The western magmatic belt is interpreted to have moved at least 800 km southward to a position outboard of the eastern magmatic belt between ca. 140 and ca. 110 Ma, which is why the southern Coast Mountains batholith is so much wider than the northern Coast Mountains batholith (Fig. 1). This sinistral motion occurred during a 140–120 Ma magmatic lull and early stages of 120–100 Ma high-flux magmatism.

High-flux magmatism between 120 and 80 Ma occurred prior to and during mid-Cretaceous accretion of the western magmatic belt (and Alexander-Wrangellia host) to the eastern belt (and Yukon-Tanana and Stikine host). Beginning ca. 100 Ma, plutons were emplaced across much of the orogen during regional metamorphism, growth/recrystallization of metamorphic zircon, crustal thickening, and west-vergent thrusting to the west and east-vergent thrusting to the east.

Late Cretaceous–Paleocene low-flux magmatism occurred in a dextral transpressional setting, and plutons were emplaced along the Coast shear zone during east-side-up reverse motion and ~150–250(?) km of dextral slip.

Eocene high-flux magmatism and rapid uplift of the axial portion of the batholiths in the northern part of the study area occurred in an extensional setting, with east-side-down normal motion along the northern Coast shear zone and the Shames mylonite zone–eastern boundary fault. Widespread growth/recrystallization of metamorphic zircon occurred during this phase of extensional tectonism. Cessation of this ca. 55–48 Ma magmatism records the demise of plate convergence along this portion of the Cordilleran margin.

APPENDIX. LEGEND FOR FIGURES 2A, 3, AND 7 AND FOR FIGURES DR1–DR3 (SEE FOOTNOTE 1)

Terranes, Terrane Boundaries, and Major Structures (From Wheeler et al. [1991] Except Where Noted)

W—Wrangellia terrane. Devonian to Permian arc volcanics, clastics, and platform carbonates; Triassic basalt and carbonate; Jurassic arc volcanics; plutons of various ages.

Boundary between Wrangellia and Alexander terranes. Interpreted to be a fault on the basis of differing geologic history.

A—Alexander terrane. Upper Proterozoic to Triassic volcanic and sedimentary rocks and comagmatic intrusions.

Boundary between Alexander terrane and Gravina belt. Interpreted to be a depositional contact on the basis of conformable relations with underlying strata of the Alexander terrane in northern part of study area.

G—Gravina belt. Upper Jurassic and Lower Cretaceous marine clastic strata and mafic to felsic volcanic rocks. Interpreted to rest depositionally on Alexander terrane and may originally have overlain Yukon-Tanana terrane (from Saleeby [2000] in southeast Alaska, Gehrels [2001] near Prince Rupert, and Gehrels [personal obs.] near Bella Coola).

Boundary between Gravina belt and Yukon-Tanana terrane. Interpreted to be a mid-Cretaceous thrust fault based on relations in Prince Rupert area (Crawford et al., 2000; Gehrels, 2001) and in southeast Alaska (Saleeby, 2000).

Y—Yukon-Tanana terrane. Upper Proterozoic(?) to Upper Paleozoic schist, gneiss, quartzite, marble, and calc-silicate, with distinctive mid-Paleozoic

metavolcanic and metaplutonic rocks. Includes Taku terrane of Saleeby (2000), Yukon-Tanana terrane of Gehrels (2001), Scotia-Quaal belt of Gareau and Woodsworth (2000), Burke Channel assemblage of Gehrels (2000), and Nisling terrane and undivided metamorphic assemblages of Wheeler et al. (1991). Probably includes rocks of the Stikine terrane in southern portions of study area.
C—Coast shear zone. Steeply east-dipping ductile shear zone with both east-side-up and east-side-down motion of latest Cretaceous–early Tertiary age.
Boundary between Yukon-Tanana and Stikine terranes. East-dipping normal fault (Shames mylonite zone [Heah, 1990, 1991; Andronicos et al., 2003] or eastern boundary detachment [Rusmore et al., 2005]) near Kitimat and Terrace; steeply east-dipping fault of uncertain net displacement near Bella Coola (Gehrels and Boghossian, 2000).
S—Stikine terrane. Devonian to Permian arc volcanics and carbonates; Triassic and Lower Jurassic arc volcanic and sedimentary rocks; plutons of various ages.

Primary Geologic Map Units (From Wheeler and McFeely [1991] Except Where Noted) Organized from Occurrence West To East

TK—Triassic Karmutsen rift volcanics in Wrangellia.
OTA—Ordovician-Triassic strata of Alexander terrane.
Sg—Silurian granodiorite and trondhjemite.
DMg, DMq—Devonian-Mississippian granitic rocks (known or suspected to be Silurian on west side of Coast Mountains; Gehrels, 2001).
MJg, MJd—Middle Jurassic diorite and granodiorite.
JKd, JKg—Late Jurassic–Early Cretaceous quartz diorite, diorite, and gabbro.
mKg, mKd, mKq, mKgE—mid-Cretaceous diorite, quartz diorite, and tonalite, locally belonging to the Ecstall pluton.
MTyk, MTg—Miocene syenite and granite.
PCN—Upper Proterozoic–Lower Cambrian metamorphosed passive continental margin assemblage (now known to be mostly mid-Paleozoic metavolcanic and metasedimentary rocks; Gareau and Woodsworth, 2000; Saleeby, 2000; Gehrels, 2001).
m, nC, mC—undivided metamorphic rocks, locally referred to as Central Gneiss Complex.
KTt—generally foliated and layered Late Cretaceous–early Tertiary quartz diorite, tonalite, and granodiorite, locally referred to as the "tonalite sill."
LKg, LKq, LKd—Late Cretaceous granodiorite, quartz diorite, and diorite.
ETg—Early Tertiary granodiorite and quartz diorite.
EJg, EJdB, EJqT—Early Jurassic granodiorite and quartz diorite, locally referred to as the Black Dome and Topley plutons.
JH—Lower and Middle Jurassic Hazelton volcanic arc complexes.
JBL—Middle and Upper Jurassic clastic strata of the Bowser Lake assemblage.
JKG—Upper Jurassic and Lower Cretaceous arc and locally rift volcanic rocks.
mKs—mid-Cretaceous volcanic and sedimentary rocks.
Ks—Cretaceous volcanic-rich clastic strata of the Skeena assemblage.
NTc—Neogene basaltic volcanic rocks of the Chilcotin assemblage.
PTK—Paleogene volcanic rocks of the Kamloops assemblage.
TQA—Tertiary and Quaternary mafic volcanic rocks of the Anahim assemblage.

ACKNOWLEDGMENTS

Funding was provided by National Science Foundation (NSF) awards EAR-9526263 and EAR-0309885 for support of the ACCRETE and BATHOLITHS projects, and by EAR-0443387 and EAR-0732436 for support of the Arizona LaserChron Center. Geochronologic analyses were conducted with the capable support of Alex Pullen, Victor Valencia, Scott Johnston, Martin Pepper, Mark Baker, David Steinke, and Jessica Bressmer of the University of Arizona. Discussions with Jason Saleeby and Scott Paterson about magmatic processes were very helpful. Axel Schmitt and Sunshine Abbott (of University of California–Los Angeles) provided invaluable assistance in the acquisition of cathodoluminescence (CL) images. Field and logistical support was provided by John Murgas (Tongass Marine) and Don Willson (Silver King Ventures). We thank Calvin Barnes and an anonymous reviewer for insightful and constructive reviews.

REFERENCES CITED

Andronicos, C.L., Hollister, L.S., Davidson, C., and Chardon, D.H., 1999, Kinematics and tectonic significance of transpressive structures within the Coast Plutonic Complex, British Columbia: Journal of Structural Geology, v. 21, p. 229–243, doi: 10.1016/S0191-8141(98)00117-5.

Andronicos, C.L., Chardon, D.H., Hollister, L.S., Gehrels, G.E., and Woodsworth, G.J., 2003, Strain partitioning in an obliquely convergent orogen, plutonism, and syn-orogenic collapse: Coast Mountains batholith, British Columbia, Canada: Tectonics, v. 22, no. 2, 24 p., doi: 10.1029/2001TC001312.

Armstrong, R.L., 1988, Mesozoic and early Cenozoic magmatic evolution of the Canadian Cordillera, *in* Clark, S.P., Burchfiel, B.C., Suppe, J., eds., Processes in continental lithospheric deformation: Geological Society of America Special Paper 218, p. 55–91.

Armstrong, R.L., and Runkle, D., 1979, Rb-Sr geochronometry of the Ecstall, Kitkiata, and Quottoon plutons and their country rocks, Prince Rupert region, Coast Plutonic Complex, British Columbia: Canadian Journal of Earth Sciences, v. 16, p. 387–399.

Arth, J.G., Barker, F., and Stern, T.W., 1988, Coast batholith and Taku plutons near Ketchikan, Alaska: Petrography, geochronology, geochemistry, and isotopic character: American Journal of Science, v. 288-A, p. 461–489.

Baer, A.J., 1973, Bella Coola–Laredo Sound Map Areas, British Columbia: Geological Survey of Canada Memoir 372, 122 p., scale 1:250,000.

Barker, F., and Arth, J.G., 1990, Two traverses across the Coast batholith, southeastern Alaska, *in* Anderson, J.L., ed., The Nature and Origin of Cordilleran Magmatism: Geological Society of America Memoir 174, p. 395–405.

Berg, H.C., Elliott, R.L., and Koch, R.D., 1988, Geologic Map of the Ketchikan and Prince Rupert Quadrangles, Southeastern Alaska: U.S. Geological Survey Miscellaneous Geologic Investigation Map I-1807, scale 1:250,000.

Boghossian, N.D., and Gehrels, G.E., 2000, Nd isotopic tracing of terranes and other sedimentary assemblages through roof pendants of the Coast Plutonic Complex between Prince Rupert and Bella Coola, British Columbia, *in* Stowell, H.H., and McClelland, W.C., eds., Tectonics of the Coast Mountains, SE Alaska and Coastal British Columbia: Geological Society of America Special Paper 343, p. 77–88.

Brew, D.A., and Ford, A.B., 1978, Megalineament in southeastern Alaska marks southwest edge of Coast Range batholithic complex: Canadian Journal of Earth Sciences, v. 15, p. 1763–1772.

Brew, D.A., and Ford, A.B., 1981, The Coast Plutonic Complex sill, southeastern Alaska, *in* Albert, N.R.D., and Hudson, T.L., eds., The U.S. Geological Survey in Alaska: Accomplishments during 1980: U.S. Geological Survey Circular 823-B, p. B96–B98.

Butler, R.F., Gehrels, G.E., Crawford, M.L., and Crawford, W.A., 2001a, Paleomagnetism of the Quottoon Plutonic Complex in the Coast Mountains of British Columbia and southeastern Alaska: Evidence for tilting during uplift: Canadian Journal of Earth Sciences, v. 38, p. 1367–1384, doi: 10.1139/cjes-38-9-1367.

Butler, R.F., Gehrels, G.E., and Kodama, K.P., 2001b, A moderate translation alternative to the Baja British Columbia hypothesis: GSA Today, v. 11, no. 6, p. 4–10, doi: 10.1130/1052-5173(2001)011<0004:AMTATT>2.0.CO;2.

Butler, R.F., Gehrels, G.E., Baldwin, S.L., and Davidson, C., 2002, Paleomagnetism and geochronology of the Ecstall pluton in the Coast Mountains of British Columbia: Evidence for local deformation rather than large-scale transport: Journal of Geophysical Research, v. 107, p. EPM 3-1–3-13.

Butler, R.F., Gehrels, G.E., Hart, W., Davidson, C., and Crawford, M.L., 2006, Paleomagnetism of Late Jurassic to mid-Cretaceous plutons near Prince Rupert, British Columbia, *in* Haggart, J.W., Enkin, R.J., and Monger, J.W.H., eds., Paleogeography of the North American Cordillera: Evidence For and Against Large-Scale Displacements: Geological Association of Canada Special Paper 46, p. 171–200.

Chardon, D., 2003, Strain partitioning and batholith emplacement at the root of a transpressive magmatic arc: Journal of Structural Geology, v. 25, no. 1, p. 91–107, doi: 10.1016/S0191-8141(02)00015-9.

Chardon, D., Andronicos, C.L., and Hollister, L.S., 1999, Large-scale transpressive shear zone patterns and displacements within magmatic arcs: The Coast Plutonic Complex, British Columbia: Tectonics, v. 18, p. 278–292, doi: 10.1029/1998TC900035.

Chen, J.H., and Moore, J.G., 1982, Uranium-lead isotopic ages from the Sierra Nevada batholith, California: Journal of Geophysical Research, v. 87, p. 4761–4784, doi: 10.1029/JB087iB06p04761.

Colpron, M., Nelson, J.L., and Murphy, D.C., 2006, A tectonostratigraphic framework for the pericratonic terranes of the northern Cordillera, *in* Colpron, M., and Nelson, J., eds., Paleozoic Evolution and Metallogeny of Pericratonic Terranes at the Ancient Pacific Margin of North America: Geological Association of Canada Special Paper 45, p. 1–23.

Cook, R.D., and Crawford, M.L., 1994, Exhumation and tilting of the western metamorphic belt of the Coast orogen in southern southeastern Alaska: Tectonics, v. 13, p. 528–537, doi: 10.1029/93TC03152.

Corfu, F., Hanchar, J.M., Hoskin, P.W.O., and Kinny, P., 2003, Atlas of zircon textures, *in* Hanchar, J.M., and Hoskin, P.W.O., eds., Zircon: Review in Mineralogy & Geochemistry, v. 53, p. 468–500.

Cowan, D.S., Brandon, M.T., and Garver, J.I., 1997, Geologic tests of hypotheses for large coastwise displacements—A critique illustrated by the Baja British Columbia controversy: American Journal of Science, v. 297, p. 117–173.

Crawford, M.L., and Hollister, L.S., 1982, Contrast of metamorphic and structural histories across the Work Channel lineament, Coast Plutonic Complex, British Columbia: Journal of Geophysical Research, v. 87, p. 3849–3860, doi: 10.1029/JB087iB05p03849.

Crawford, M.L., Hollister, L.S., and Woodsworth, G.J., 1987, Crustal deformation and regional metamorphism across a terrane boundary, Coast Plutonic Complex, British Columbia: Tectonics, v. 6, p. 343–361, doi: 10.1029/TC006i003p00343.

Crawford, M.L., Klepeis, K.A., Gehrels, G.E., and Isachsen, C.E., 1999, Batholith emplacement at mid-crustal levels and its exhumation within an obliquely convergent margin: Tectonophysics, v. 312, p. 57–78, doi: 10.1016/S0040-1951(99)00170-5.

Crawford, M.L., Crawford, W.C., and Gehrels, G.E., 2000, Metasedimentary rocks of the Prince Rupert area, coastal British Columbia, *in* Stowell, H.H., and McClelland, W.C., eds., Tectonics of the Coast Mountains, SE Alaska and Coastal British Columbia: Geological Society of America Special Paper 343, p. 1–22.

Crawford, M.L., Crawford, W.C., and Lindline, J., 2005, 105 million years of igneous activity, Wrangell, Alaska to Prince Rupert, British Columbia: Canadian Journal

of Earth Sciences, v. 42, p. 1097–1116, doi: 10.1139/e05-022.

Crawford, M.L., Klepeis, K.A., Gehrels, G.E., and Lindline, J., 2009, Mid-Cretaceous–Recent crustal evolution in the central Coast orogen, British Columbia and southeastern Alaska, *in* Miller, R.B., and Snoke, A.W., eds., Crustal Cross-Sections from the Western North American Cordillera and Elsewhere: Implications for Tectonic and Petrologic Processes: Geological Society of America Special Paper (in press).

Currie, L.D., and Parrish, R.R., 1997, Paleozoic and Mesozoic rocks of Stikinia exposed in northwestern British Columbia: Implications for correlations in the northern Cordillera: Geological Society of America Bulletin, v. 109, p. 1402–1420, doi: 10.1130/0016-7606(1997)109<1402:PAMROS>2.3.CO;2.

Davidson, C., Davis, K.J., Bailey, C.M., Tape, C.H., Singleton, J., and Singer, B., 2003, Age, origin, and significance of brittle faulting and pseudotachylyte along the Coast shear zone, Prince Rupert, British Columbia: Geology, v. 31, p. 43–46, doi: 10.1130/0091-7613(2003)031<0043:AOASOB>2.0.CO;2.

DeGraaff-Surpless, K., Mahoney, J.B., Wooden, J.L., and McWilliam, M.O., 2003, Lithofacies control in detrital zircon provenance studies: Insights from the Cretaceous Methow Basin, southern Canadian Cordillera: Geological Society of America Bulletin, v. 115, no. 8, p. 899–915, doi: 10.1130/B25267.1.

de Silva, S., and Gosnold, W.D., 2007, Episodic construction of batholiths: Insights from the spatio-temporal development of an ignimbrite flare-up: Journal of Volcanology and Geothermal Research, v. 167, p. 320–335, doi: 10.1016/j.jvolgeores.2007.07.015.

Diakow, L.J., 2006, Geology of the Tahtsa Ranges between Eutsuk Lake and Morice Lake, Whitesail Lake Map Area, West-Central British Columbia: British Columbia Geological Survey Geoscience Map 2006–5, scale 1:150,000.

Douglas, B.J., 1986, Deformational history of an outlier of metasedimentary rocks, Coast Plutonic Complex, British Columbia, Canada: Canadian Journal of Earth Sciences, v. 23, p. 813–826.

Ducea, M.N., and Barton, M.D., 2007, Igniting flare-up events in Cordilleran arcs: Geology, v. 35, p. 1047–1050, doi: 10.1130/G23898A.1.

Engebretson, D.C., Cox, A., and Gordon, R.G., eds., 1985, Relative Motions between Oceanic and Continental Plates in the Pacific Basin: Geological Society of America Special Paper 206, 59 p.

Evenchick, C.A., 1991, Geometry, evolution, and tectonic framework of the Skeena fold belt, north central British Columbia: Tectonics, v. 10, no. 3, p. 527–546, doi: 10.1029/90TC02680.

Farley, K.A., Rusmore, M.E., and Bogue, S.W., 2001, Post–10 Ma uplift and exhumation of the northern Coast Mountains, British Columbia: Geology, v. 29, p. 99–102, doi: 10.1130/0091-7613(2001)029<0099:PMUAEO>2.0.CO;2.

Friedman, R.M., and Armstrong, R.L., 1995, Jurassic and Cretaceous geochronology of the southern Coast belt, British Columbia, 49° to 51°N, *in* Miller, D.M., and Busby, C., eds., Jurassic Magmatism and Tectonics of the North American Cordillera: Geological Society of America Special Paper 299, p. 95–139.

Friedman, R.M., and Mortensen, J.K., 2002, U-Pb zircon and titanite dating in support of British Columbia Geological Survey regional mapping studies, *in* Geological Fieldwork 2001: British Columbia Ministry of Energy and Mines Paper 2002–1, p. 135–149.

Friedman, R.M., Gareau, S.A., and Woodsworth, G.J., 2001, U-Pb dates from the Scotia-Quaal metamorphic belt, Coast Plutonic Complex, central-western British Columbia: Geological Survey of Canada Current Research 2001–F9, Report 14, p. 1–7.

Gabrielse, H., Murphy, D.C., and Mortensen, J.K., 2006, Cretaceous and Cenozoic dextral orogen-parallel displacements, magmatism, and paleogeography, north-central Canadian Cordillera, *in* Haggart, J.W., Enkin, R.J., and Monger, J.W.H., eds., Paleogeography of the North American Cordillera: Evidence For and Against Large-Scale Displacements: Geological Association of Canada Special Paper 46, p. 255–276.

Gareau, S.A., 1989, Metamorphism, deformation, and geochronology of the Ecstall-Quall Rivers area, Coast Plutonic Complex, British Columbia: Geological Survey of Canada Paper 89–1E, p. 155–162.

Gareau, S.A., 1991a, Geology of the Scotia-Quaal Metamorphic Belt, Coast Plutonic Complex, British Columbia [Ph.D. thesis]: Ottawa, Canada, Carleton University, 390 p.

Gareau, S.A., 1991b, Geology of the Scotia-Quaal Metamorphic Belt, Coast Plutonic Complex, British Columbia: Geological Survey of Canada Open-File Map 2337, scale 1:50,000, 4 sheets.

Gareau, S.A., 1991c, The Scotia-Quaal metamorphic belt: A distinct assemblage with pre–early Late Cretaceous deformational and metamorphic history, Coast Plutonic Complex, British Columbia: Canadian Journal of Earth Sciences, v. 28, p. 870–880.

Gareau, S.A., and Woodsworth, G.J., 2000, Yukon-Tanana terrane in the Scotia-Quaal belt, Coast Plutonic Complex, central-western British Columbia, *in* Stowell, H.H., and McClelland, W.C., eds., Tectonics of the Coast Mountains, SE Alaska and Coastal British Columbia: Geological Society of America Special Paper 343, p. 23–43.

Gareau, S.A., Friedman, R.M., Woodsworth, G.J., and Childe, F., 1997, U-Pb ages from the northeastern quadrant of Terrace map area, west-central British Columbia: Geological Survey of Canada Current Research 1997-A, p. 31–40.

Gehrels, G.E., 2000a, Introduction to detrital zircon studies of Paleozoic and Triassic strata in western Nevada and northern California, *in* Soreghan, M.J., and Gehrels, G.E., eds., Paleozoic and Triassic Paleogeography and Tectonics of Western Nevada and Northern California: Geological Society of America Special Paper 347, p. 1–18.

Gehrels, G.E., 2000b, Reconnaissance geology and U-Pb geochronology of the western flank of the Coast Mountains between Juneau and Skagway, southeastern Alaska, *in* Stowell, H.H., and McClelland, W.C., eds., Tectonics of the Coast Mountains, SE Alaska and Coastal British Columbia: Geological Society of America Special Paper 343, p. 213–234.

Gehrels, G.E., 2001, Geology of the Chatham Sound region, southeast Alaska and coastal British Columbia: Canadian Journal of Earth Sciences, v. 38, p. 1579–1599, doi: 10.1139/cjes-38-11-1579.

Gehrels, G.E., and Boghossian, N.D., 2000, Reconnaissance geology and U-Pb geochronology of the west flank of the Coast Mountains between Bella Coola and Prince Rupert, coastal British Columbia, *in* Stowell, H.H., and McClelland, W.C., eds., Tectonics of the Coast Mountains, SE Alaska and Coastal British Columbia: Geological Society of America Special Paper 343, p. 61–76.

Gehrels, G.E., and McClelland, W.C., 1988, Early Tertiary uplift of the Coast Range batholith along west-side-up extensional shear zones: Geological Society of America Abstracts with Programs, v. 21, p. A111.

Gehrels, G.E., McClelland, W.C., Samson, S.D., Patchett, P.J., and Brew, D.A., 1991, U-Pb geochronology of Late Cretaceous and early Tertiary plutons of the northern Coast Mountains batholith: Canadian Journal of Earth Sciences, v. 28, p. 899–911.

Gehrels, G.E., McClelland, W.C., Samson, S.D., Patchett, P.J., and Orchard, M.J., 1992, Geology of the western flank of the Coast Mountains between Cape Fanshaw and Taku Inlet, southeastern Alaska: Tectonics, v. 11, p. 567–585, doi: 10.1029/92TC00482.

Gehrels, G.E., Valencia, V.A., and Ruiz, J., 2008, Enhanced precision, accuracy, efficiency, and spatial resolution of U-Th-Pb ages by LA-MC-ICPMS: Geochemistry, Geophysics, Geosystems, v. 9, p. Q03017, doi: 10.1029/2007GC001805.

Haeussler, P., Bradley, D., Wells, R., and Miller, M., 2003, Life and death of the Resurrection plate: Evidence for its existence and subduction in the northeastern Pacific in Paleocene-Eocene time: Geological Society of America Bulletin, v. 115, no. 7, p. 867–880, doi: 10.1130/0016-7606(2003)115<0867:LADOTR>2.0.CO;2.

Haggart, J.W., Diakow, L.J., Mahoney, J.B., Woodsworth, G.J., Struik, L.S., Gordee, S.M., and Rusmore, M., 2006a, Geology, Bella Coola region (NTS 93D/01, /07, /08, /10, /15, and parts of 93D/02, /03, /06, /09, /11, /14, /16, and 92M/15 and /16), British Columbia: Geological Survey of Canada Open-File 5385, and British Columbia Geological Survey Geoscience Map 2006–7, 3 sheets, scale 1:100,000.

Haggart, J.W., Woodsworth, G.J., and McNicoll, V.J., 2006b, Uranium-Lead Geochronology of Two Intrusions in the Southern Bowser Basin, British Columbia: Geological Survey of Canada Current Research 2006–F2, 6 p.

Haggart, J.W., Diakow, L.J., Mahoney, J.B., Woodsworth, G.J., Struik, L.C., Gordee, S.M., Israel, S., Hooper, R.L., van der Heyden, P., Rusmore, M., Lett, R., Ceh, M., Hastings, N.L., and Wagner, C., 2007, Bedrock Geology, Bella Coola Region (93C, 93D, 93E, 92M, and 92N), British Columbia: Geological Survey of Canada Open-File 5410, CD.

Harley, S., Kelly, N., and Moller, A., 2007, Zircon behavior and the thermal histories of mountain chains: Elements, v. 3, p. 25–30, doi: 10.2113/gselements.3.1.25.

Harrison, T.M., Armstrong, R.L., Naesser, C.W., and Harakal, J.E., 1979, Geochronology and thermal history of the Coast Plutonic Complex, near Prince Rupert, British Columbia: Canadian Journal of Earth Sciences, v. 16, p. 400–410.

Heah, T.S.T., 1990, Eastern margin of the Central Gneiss Complex in the Shames River area, Terrace, British Columbia, *in* Current Research, Part E: Geological Survey of Canada Paper 90–1E, p. 159–169.

Heah, T.S.T., 1991, Mesozoic Ductile Shear and Paleogene Extension along the Eastern Margin of the Central Gneiss Complex, Coast Belt, Shames River Area, Near Terrace, British Columbia [M.S. thesis]: Vancouver, University of British Columbia, 155 p.

Hill, M.L., 1985, Remarkable fossil locality: Crinoid stems from migmatite of the Coast Plutonic Complex, British Columbia: Geology, v. 13, p. 825–826, doi: 10.1130/0091-7613(1985)13<825:RFLCSF>2.0.CO;2.

Himmelberg, G.R., Haeussler, P.J., and Brew, D.A., 2004, Emplacement, rapid burial, and exhumation of 90-Ma plutons in southeastern Alaska: Canadian Journal of Earth Sciences, v. 41, p. 87–102, doi: 10.1139/e03-087.

Hollister, L.S., 1982, Metamorphic evidence for rapid (2 mm/yr) uplift of a portion of the Central Gneiss Complex, Coast Mountains, B.C: Canadian Mineralogist, v. 20, p. 319–332.

Hollister, L.S., and Andronicos, C., 1997, A candidate for the Baja British Columbia fault system in the Coast Plutonic Complex: GSA Today, v. 7, no. 11, p. 1–7.

Hollister, L.S., and Andronicos, C., 2000, The Central Gneiss Complex, Coast Mountains, British Columbia, *in* Stowell, H.H., and McClelland, W.C., eds., Tectonics of the Coast Mountains, SE Alaska and British Columbia: Geological Society of America Special Paper 343, p. 45–59.

Hollister, L.S., and Andronicos, C., 2006, Formation of new continental crust in Western British Columbia during transpression and transtension: Earth and Planetary Science Letters, v. 249, p. 29–38, doi: 10.1016/j.epsl.2006.06.042.

Hollister, L.S., and Crawford, M.L., 1986, Melt-enhanced deformation: A major tectonic process: Geology, v. 14, p. 558–561, doi: 10.1130/0091-7613(1986)14<558:MDAMTP>2.0.CO;2.

Hollister, L.S., Grissom, G.C., Peters, E.K., Stowell, H.H., and Sisson, V.B., 1987, Confirmation of the empirical correlation of aluminum in hornblende with pressure of solidification of calcalkaline plutons: The American Mineralogist, v. 72, p. 231–239.

Hollister, L.S., Hargraves, R.B., James, T.S., and Renne, P.R., 2004, The paleomagnetic effects of reheating the Ecstall pluton, British Columbia: Earth and Planetary Science Letters, v. 221, p. 397–407, doi: 10.1016/S0012-821X(04)00067-6.

Hoskin, P., and Schaltegger, U., 2003, The composition of zircon and igneous and metamorphic petrogenesis, *in* Hanchar, J., and Hoskin, P., eds., Zircon: Reviews of Mineralogy and Geochemistry, v. 53, p. 27–62.

Hutchison, W.W., 1982, Geology of the Prince Rupert–Skeena Map Area, British Columbia: Geological Survey of Canada Memoir 394, 116 p.

Hutchison, W., Berg, H., and Okulitch, A., 1973, Skeena River, Sheet 103: Geological Survey of Canada Map 1385A, scale 1:1,000,000.

Ingram, G.M., and Hutton, D.H.W., 1994, The great tonalite sill: Emplacement into a contractional shear zone and implications for Late Cretaceous to early Eocene tectonics in southeastern Alaska and British Columbia: Geological Society of America Bulletin, v. 106, p. 715–728, doi: 10.1130/0016-7606(1994)106<0715:TGTSEI>2.3.CO;2.

Johnston, S., Gehrels, G., Valencia, V., and Ruiz, J., 2009, Small-volume U-Pb geochronology by laser-ablation-multicollector-ICPMS: Chemical Geology (in press).

Klepeis, K.A., and Crawford, M.L., 1999, High-temperature arc-parallel normal faulting and transtension at the roots of an obliquely convergent orogen: Geology, v. 27, p. 7–10, doi: 10.1130/0091-7613(1999)027<0007:HTAPNF>2.3.CO;2.

Klepeis, K.A., Crawford, M.L., and Gehrels, G.E., 1998, Structural history of the crustal-scale Coast shear zone north of Portland Canal, southeast Alaska and British Columbia: Journal of Structural Geology, v. 20, p. 883–904, doi: 10.1016/S0191-8141(98)00020-0.

Lanphere, M.L., 1978, Displacement history of the Denali fault system, Alaska and Canada: Canadian Journal of Earth Sciences, v. 15, p. 817–822.

Lowey, G., 2007, Lithofacies analysis of the Dezadeash Formation (Jura–Cretaceous), Yukon, Canada: The depositional architecture of a mud/sand-rich turbidite system: Sedimentary Geology, v. 198, p. 273–291, doi: 10.1016/j.sedgeo.2006.12.011.

Ludwig, K.R., 2003, Isoplot 3.00: Berkeley Geochronology Center Special Publication 4, 70 p.

Mahoney, J.B., Haggart, J.W., Woodsworth, G.J., Hooper, R.L., and Snyder, L.S., 2007a, Geology, Kitlope Lake (east part) (93E/04), British Columbia: Geological Survey of Canada Open-File 5588, and Geoscience British Columbia Map 2007–11–4, 1 sheet, scale 1:50,000.

Mahoney, J.B., Haggart, J.W., Hooper, R.L., Snyder, L.S., and Woodsworth, G.J., 2007b, Geology, Tsaytis River (93E/05), British Columbia: Geological Survey of Canada Open-File 5587, and Geoscience British Columbia Map 2007–11–3, 1 sheet, scale 1:50,000.

Mahoney, J.B., Haggart, J.W., Hooper, R.L., Snyder, L.S., and Woodsworth, G.J., 2007c, Geology, parts of Chikamin Mountain and Troitsa Lake (93E/06, 11), British Columbia: Geological Survey of Canada Open-File 5586, and Geoscience British Columbia Map 2007–11–2, 1 sheet, scale 1:50,000.

Mahoney, J.B., Haggart, J.W., Hooper, R.L., Snyder, L.S., and Woodsworth, G.J., 2007d, Geology, Tahtsa Peak (93E/12), British Columbia: Geological Survey of Canada Open-File 5585, and Geoscience British Columbia Map 2007–11–1, 1 sheet, scale 1:50,000.

Mahoney, J.B., Hooper, R.L., Gordee, S.M., and Haggart, J.W., 2007e, Geology, Foresight Mountain (93E/03), British Columbia: Geological Survey of Canada Open-File 5386 (revised), and Geoscience British Columbia Map 2006–2, 1 sheet, scale 1:50,000.

Mahoney, J.B., Gordee, S.M., Haggart, J.W., Friedman, R.M., Diakow, L.J., and Woodsworth, G.J., 2009, Magmatic evolution of the eastern Coast Plutonic Complex, Bella Coola region, west-central British Columbia: Geological Society of America Bulletin (in press).

Mattinson, J.M., 1982, U-Pb "blocking temperatures" and Pb loss characteristics in young zircon, sphene, and apatite: Geological Society of America Abstracts with Programs, v. 14, p. 558.

McClelland, W.C., Gehrels, G.E., Samson, S.D., and Patchett, P.J., 1992a, Structural and geochronologic relations along the western flank of the Coast Mountains batholith: Stikine River to Cape Fanshaw, central southeastern Alaska: Journal of Structural Geology, v. 14, p. 475–489, doi: 10.1016/0191-8141(92)90107-8.

McClelland, W.C., Gehrels, G.E., and Saleeby, J.B., 1992b, Upper Jurassic–Lower Cretaceous basinal strata along the Cordilleran margin: Implications for the accretionary history of the Alexander-Wrangellia-Peninsular terrane: Tectonics, v. 11, p. 823–835, doi: 10.1029/92TC00241.

Mihalynuk, M.G., Nelson, J., and Diakow, L.J., 1994, Cache Creek terrane entrapment: Oroclinal paradox within the Canadian Cordillera: Tectonics, v. 13, p. 575–595, doi: 10.1029/93TC03492.

Miller, I.M., Brandon, M.T., and Hickey, L.J., 2006, Using leaf margin analysis to estimate the mid-Cretaceous (Albian) paleolatitude of the Baja BC block: Earth and Planetary Science Letters, v. 245, p. 95–114, doi: 10.1016/j.epsl.2006.02.022.

Monger, J.W.H., Price, R.A., and Tempelman-Kluit, D.J., 1982, Tectonic accretion and the origin of the two major metamorphic welts in the Canadian Cordillera: Geology, v. 10, p. 70–75, doi: 10.1130/0091-7613(1982)10<70:TAATOO>2.0.CO;2.

Monger, J.W.H., van der Heyden, P., Journeay, J.M., Evenchick, C.A., and Mahoney, J.B., 1994, Jurassic-Cretaceous basins along the Canadian Coast belt: Their bearing on pre–mid-Cretaceous sinistral displacements: Geology, v. 22, p. 175–178, doi: 10.1130/0091-7613(1994)022<0175:JCBATC>2.3.CO;2.

Morozov, I.B., Smithson, S.B., Hollister, L.S., and Diebold, J.B., 1998, Wide-angle seismic imaging across accreted terranes, southeastern Alaska and western British Columbia: Tectonophysics, v. 299, p. 281–296, doi: 10.1016/S0040-1951(98)00208-X.

Morozov, I.B., Smithson, S.B., Chen, J., and Hollister, L.S., 2001, Generation of new continental crust and terrane accretion in southeastern Alaska and western British Columbia: Constraints from P- and S- wave wide-angle data (ACCRETE): Journal of Geophysical Research, v. 341, p. 49–67.

Parrish, R.R., 1983, Cenozoic thermal evolution and tectonics of the Coast Mountains of British Columbia: 1. Fission track dating, apparent uplift rates, and patterns of uplift: Tectonics, v. 2, p. 601–631, doi: 10.1029/TC002i006p00601.

Patchett, P.J., Gehrels, G.E., and Isachsen, C.E., 1998, Nd isotopic characteristics of metamorphic and plutonic rocks of the Coast Mountains near Prince Rupert, British Columbia: Canadian Journal of Earth Sciences, v. 35, p. 556–561, doi: 10.1139/cjes-35-5-556.

Pidgeon, R.T., Bosch, D., and Bruguier, O., 1996, Inherited zircon and titanite U-Pb systems in an Archaean syenite from southwestern Australia: Implications for U-Pb stability of titanite: Earth and Planetary Science Letters, v. 141, p. 187–198, doi: 10.1016/0012-821X(96)00068-4.

Ridgway, K.D., Trop, J.M., Nokleberg, W.J., Davidson, C., and Eastham, K.R., 2002, Mesozoic and Cenozoic tectonics of the eastern and central Alaska Range: Progressive basin development and deformation in a suture zone: Geological Society of America Bulletin, v. 114, p. 1480–1504, doi: 10.1130/0016-7606(2002)114<1480:MACTOT>2.0.CO;2.

Roddick, J.A., 1970, Douglas Channel–Hecate Strait Map-Area, British Columbia: Geological Survey of Canada Paper 70–41, 56 p., scale 1:250,000.

Roddick, J.A., 1983, Geophysical review and composition of the Coast Plutonic Complex, south of latitude 55°N, *in* Roddick, J.A., ed., Circum-Pacific plutonic terranes: Geological Society of America Memoir 159, p. 195–211.

Roddick, J.A., 1994, Rivers Inlet (92M)–Queens Sound (102P) Map Areas: Geological Survey of Canada Open-File 2787, scale 1:250,000.

Roddick, J.A., and Hutchison, W.W., 1974, Setting of the Coast Plutonic Complex, British Columbia: Pacific Geology, v. 8, p. 91–108.

Rubatto, D., 2002, Zircon trace element geochemistry: Partitioning with garnet and the link between U-Pb ages and metamorphism: Chemical Geology, v. 184, p. 123–138, doi: 10.1016/S0009-2541(01)00355-2.

Rubatto, D., Williams, I., and Buck, I., 2001, Zircon and monazite response to prograde metamorphism in the Reynolds Range, central Australia: Contributions to Mineralogy and Petrology, v. 140, p. 458–468, doi: 10.1007/PL00007673.

Rubin, C.M., Saleeby, J.B., Cowan, D.S., Brandon, M.T., and McGroder, M.F., 1990, Regionally extensive mid-Cretaceous west-vergent thrust system in the northwestern Cordillera: Implications for continent-margin tectonism: Geology, v. 18, p. 276–280, doi: 10.1130/0091-7613(1990)018<0276:REMCWV>2.3.CO;2.

Rusmore, M.E., and Woodsworth, G.J., 1991, Coast Plutonic Complex: A mid-Cretaceous contractional orogen: Geology, v. 19, p. 941–944, doi: 10.1130/0091-7613(1991)019<0941:CPCAMC>2.3.CO;2.

Rusmore, M.E., Woodsworth, G.J., and Gehrels, G.E., 2000, Structural history of the Sheemahant shear zone, southwest of Bella Coola, British Columbia, and implications for the Late Cretaceous evolution of the Coast orogen, *in* Stowell, H.H., and McClelland, W.C., eds., Tectonics of the Coast Mountains, SE Alaska and Coastal British Columbia: Geological Society of America Special Paper 343, p. 89–106.

Rusmore, M.E., Gehrels, G.E., and Woodsworth, G.J., 2001, Southern continuation of the Coast shear zone and Paleocene strain partitioning in British Columbia–southeast Alaska: Geological Society of America Bulletin, v. 113, p. 961–975, doi: 10.1130/0016-7606(2001)113<0961:SCOTCS>2.0.CO;2.

Rusmore, M.E., Woodsworth, G.J., and Gehrels, G.E., 2005, Two-stage exhumation of midcrustal arc rocks, Coast Mountains, British Columbia: Tectonics, v. 24, 25 p., doi: 10.1029/2004TC001750.

Saleeby, J.B., 2000, Geochronologic investigations along the Alexander-Taku terrane boundary, southern Revillagigedo Island to Cape Fox areas, southeast Alaska, *in* Stowell, H.H., and McClelland, W.C., eds., Tectonics of the Coast Mountains in SE Alaska and Coastal British Columbia: Geological Society of America Special Paper 343, p. 107–143.

Samson, S.D., McClelland, W.C., Patchett, P.J., and Gehrels, G.E., 1991a, Nd and Sr isotopic constraints on the petrogenesis of the west side of the northern Coast Mountains batholith, Alaskan and Canadian Cordillera: Canadian Journal of Earth Sciences, v. 28, p. 939–946.

Samson, S.D., Patchett, P.J., McClelland, W.C., and Gehrels, G.E., 1991b, Nd isotopic characterization of metamorphic rocks in the Coast Mountains, Alaskan and Canadian Cordillera: Ancient crust bounded by juvenile terranes: Tectonics, v. 10, p. 770–780, doi: 10.1029/90TC02732.

Smith, T.E., Riddle, C., and Jackson, T.A., 1979, Chemical variation within the Coast Plutonic Complex of British Columbia between lat 53° and 55°N: Geological Society of America Bulletin, v. 90, p. 346–356, doi: 10.1130/0016-7606(1979)90<346:CVWTCP>2.0.CO;2.

Stacey, J.S., and Kramers, J.D., 1975, Approximation of terrestrial lead evolution by a two-stage model: Earth and Planetary Science Letters, v. 26, p. 207–221, doi: 10.1016/0012-821X(75)90088-6.

Stowell, H.H., and Crawford, M.L., 2000, Metamorphic history of the Coast Mountains orogen, western British Columbia and southeastern Alaska, *in* Stowell, H.H., and McClelland, W.C., eds., Tectonics of the Coast Mountains, SE Alaska and British Columbia: Geological Society of America Special Paper 343, p. 257–284.

Stowell, H.H., and Hooper, R.J., 1990, Structural development of the western metamorphic belt adjacent to the Coast Plutonic Complex, evidence from Holkham Bay: Tectonics, v. 9, p. 391–407, doi: 10.1029/TC009i003p00391.

Tarduno, T., Duncan, R., Scholl, D., Cottrell, R., Steinberger, B., Thordarson, T., Kerr, B., Neal, C., Frey, F., Torii, M., and Carvallo, C., 2003, The Emperor Seamounts: Southward motion of the Hawaiian hotspot plume in Earth's mantle: Science, v. 301, p. 1064–1069, doi: 10.1126/science.1086442.

Thomas, J.B., and Sinha, A.K., 1999, Field, geochemical, and isotopic evidence for magma mixing and assimilation and fractional crystallization processes in the Quottoon igneous complex, northwestern British Columbia and southeastern Alaska: Canadian Journal of Earth Sciences, v. 36, p. 819–831, doi: 10.1139/cjes-36-5-819.

Tipper, H., Campbell, R., Taylor, G., and Stott, D., 1974, Parsnip River, Sheet 93: Geological Survey of Canada Map 1424A, scale 1:1,000,000.

Twenhofel, W.S., and Sainsbury, C.L., 1958, Fault patterns in southeastern Alaska: Geological Society of America Bulletin, v. 69, p. 1431–1442, doi: 10.1130/0016-7606(1958)69[1431:FPISA]2.0.CO;2.

van der Heyden, P., 1989, U-Pb and K-Ar Geochronometry of the Coast Plutonic Complex, 53°N to 54°N, British Columbia, and Implications for the Insular-Intermontane Superterrane Boundary [Ph.D. dissertation]: Vancouver, University of British Columbia, 392 p.

van der Heyden, P., 1992, A Middle Jurassic to early Tertiary Andean-Sierran arc model for the Coast belt of British Columbia: Tectonics, v. 11, p. 82–97, doi: 10.1029/91TC02183.

van der Heyden, P., 2004, Uranium-Lead and Potassium-Argon Ages from Eastern Bella Coola and Adjacent Parts of Anahim Lake and Mount Waddington Map Areas, West-Central British Columbia: Geological Survey of Canada Current Research 2004–A2, 14 p.

Wheeler, J.O., and McFeely, P., 1991, Tectonic Assemblage Map of the Canadian Cordillera: Geological Survey of Canada Map 1712A, scale 1:2,000,000.

Wheeler, J.O., Brookfield, A.J., Gabrielse, H., Monger, J.W.H., Tipper, H.W., and Woodsworth, G.J., 1991, Terrane Map of the Canadian Cordillera: Geological Survey of Canada Map 1713A, scale 1:2,000,000.

Williams, I., 2001, Response of detrital zircon and monazite, and their U-Pb isotopic systems, to regional metamorphism and host-rock partial melting, Cooma complex, southeastern Australia: Australian Journal of Earth Sciences, v. 48, p. 557–580, doi: 10.1046/j.1440-0952.2001.00883.x.

Woodsworth, G.J., Anderson, R.G., and Armstrong, R.L., 1992, Plutonic regimes, *in* Gabrielse, H., and Yorath, C. J., eds., Geology of the Cordilleran Orogen in Canada: Ottawa, Canada, Geological Survey of Canada, Geology of Canada, no. 4, p. 491–531.

Wyld, S.J., Umhoefer, P.J., and Wright, J.E., 2006, Reconstructing northern Cordilleran terranes along known Cretaceous and Cenozoic strike-slip faults: Implications for the Baja British Columbia hypothesis and other models, *in* Haggart, J.W., Enkin, R.J., and Monger, J.W.H., eds., Paleogeography of the North American Cordillera: Evidence For and Against Large-Scale Displacements: Geological Association of Canada Special Paper 46, p. 277–298.

Zen, E-an, 1985, Implications of magmatic epidote-bearing plutons on crustal evolution in the accreted terranes of northwestern North America: Geology, v. 13, p. 266–269.

Zen, E-an, and J.M. Hammarstrom, 1984, Magmatic epidote and its petrologic significance: Geology, v. 12, p. 515–518.

Manuscript Received 8 January 2008
Revised Manuscript Received 6 October 2008
Manuscript Accepted 30 October 2008

Printed in the USA